Journal of Medicinal Chemistry

Article

Discovery and Lead Optimization of Atropisomer D1 Agonists with Reduced Desensitization

Jennifer E. Davoren, Deane M Nason, Jotham Coe, Keith Dlugolenski, Christopher J. Helal, Anthony R. Harris, Erik LaChapelle, Sidney Liang, Yue Liu, Rebecca E O'Connor, Christine C Orozco, Brajesh Kumar Rai, Michelle Salafia, Brian M. Samas, Wenjian Xu, Rouba Kozak, and David Gray

J. Med. Chem., **Just Accepted Manuscript** • DOI: 10.1021/acs.jmedchem.8b01622 • Publication Date (Web): 15 Nov 2018

Just Accepted

ACS Publications

is published by the American Chemical Society. 1155 Sixteenth Street N.W., Washington, DC 20036

Discovery and Lead Optimization of Atropisomer D1 Agonists with Reduced Desensitization

Jennifer E. Davoren,*† Deane Nason,‡ Jotham Coe,‡ Keith Dlugolenski,§ Christopher Helal,‡ Anthony R. Harris,‡ Erik LaChapelle,‡ Sidney Liang,‡ Yue Liu,§ Rebecca O'Connor,‡ Christine C. Orozco,‡ Brajesh Rai,† Michelle Salafia,‡ Brian Samas,‡ Wenjian Xu,‡ Rouba Kozak,§ and David Gray§

†Medicine Design & §Internal Medicine Research Unit, Pfizer Worldwide Research and Development, 610 Main Street, Cambridge, Massachusetts 02139, United States; ‡Medicine Design, Pfizer Worldwide Research and Development, Eastern Point Road, Groton, Connecticut 06340, United States

ADDRESS: Pfizer, 610 Main Street, Cambridge, Massachusetts 02139

KEYWORDS: Dopamine receptor; GPCR, partial agonist; biased signaling, cAMP, β-arrestin, desensitization, Parkinson's disease, schizophrenia, atropisomer, D1; D1R; hit to lead, high-throughput screen, ligand-based drug optimization.

Abstract

The discovery of D1 subtype-selective agonists with drug-like properties has been an enduring challenge for the greater part of 40 years. All known D1-selective agonists are catecholamines which bring about receptor desensitization and undergo rapid metabolism thus limiting their

utility as a therapeutic for chronic illness such as Schizophrenia and Parkinson's disease. Our high-throughput screening efforts on D1 yielded a single non-catecholamine hit, PF-4211 (**6**) that was developed into a series of potent D1 receptor agonist leads with high oral bioavailability and CNS penetration. An important structural feature of this series is the locked biaryl ring system resulting in atropisomerism. Disclosed herein is a summary of our hit-to-lead efforts on this series of D1 activators culminating in the discovery of atropisomer **31** (PF-06256142), a potent and selective orthosteric agonist of the D1 receptor that has reduced receptor desensitization relative to dopamine and other catechol-containing agonists.

Introduction:

The dopamine (DA) receptors are a family of five G protein-coupled receptors (GPCRs) expressed throughout the nervous system.[1] Based on their pharmacological profiles, localization, and mechanism of action, they are roughly characterized as either D1-like (D1 and D5) or D2-like (D2, D3 and D4).[2] Activated D1-like receptors signal via the G_s subunit which increases intracellular cAMP,[3] while D2 receptors signal through G_i, which decreases cAMP levels in the cell. D1 receptors play a central role in synaptic plasticity, basal ganglia-mediated motor function, and specific domains of cognitive function including spatial learning and memory, reversal learning, extinction learning, and incentive learning.[4] D1 receptor signaling is deficient in a variety of psychiatric, neurological, and endocrine disorders such as Parkinson's disease (PD)[5] and schizophrenia.[6]

Development of a D1-selective (vs. D2) activator with properties suitable for oral administration has been an enduring challenge for medicinal chemists for over 40 years.[7] Benzodiazepine and benzoquinoline orthosteric agonist chemical series (Figure 1) have been at the forefront of published D1-selective chemical matter for decades.[8] Both of these chemical

series, as well as other known D1-selective agonists,[9] are based on a dopamine-containing core, and retain the amine and catechol functionalities (blue) of the native ligand. A hallmark of these chemical series is impaired brain penetration; additionally, rapid in vivo clearance following bioconjugation, mediated by systems which specifically recognize and metabolize the catechol moiety, further hampers the development of this chemotype.[8c, 10]

An impressive number of medicinal chemistry efforts have been specifically directed toward identifying clinically viable compounds[11] but, to date, the only D1-selective agent to reach the market is Fenoldopam (**5**) (Figure 1),[12] a rapid-acting, peripherally restricted[13] vasodilator that is dosed intravenously (IV) to treat acute hypertensive crisis.[14] Despite these challenges, the D1 system remains an attractive therapeutic target.

Herein we describe the screening and medicinal chemistry strategies which led to the identification and optimization of a novel series of non-catecholamine D1-orthosteric agonists that are both orally bioavailable[15] and CNS-penetrant. Lead examples from this series have an asymmetric sterically hindered bi-aryl bond and exist as stable atropisomer enantiomers. These ligands display robust activity in vivo and evidence of significantly reduced D1 receptor desensitization and recruitment of β-arrestin relative to dopamine and other catechol-containing agonists. This pharmacology profile was unanticipated, but is well suited for the treatment of chronic diseases, such as schizophrenia and Parkinson's disease where the duration of therapeutic effect is an important component of patient quality of life.

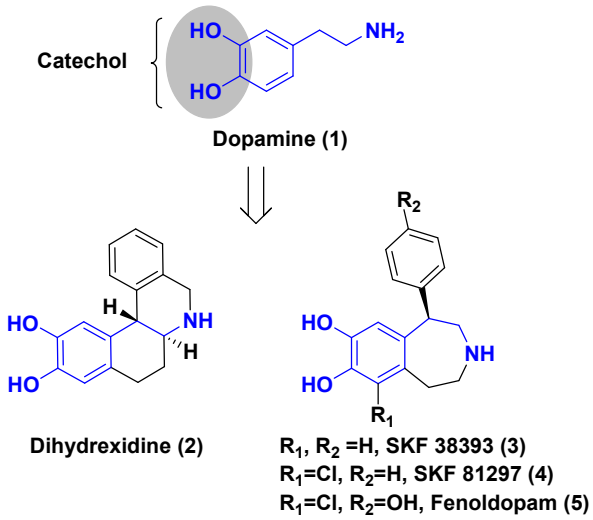

Figure 1: Representative early medicinal chemistry efforts, based on a modified dopamine scaffold, for achieving D1 vs D2 selectivity. The embedded phenethylamine group (blue) is required for binding and agonism.

Results and Discussion

Screening: Available literature suggested that potent and even modestly selective activators of D1 that lack the catecholamine motif are rare, although recent reports by Bristol-Myers Squibb[16] and Astellas Pharma[17] have disclosed the discovery of non-catecholamine D1-selective positive allosteric modulators (PAMs). In our effort to identify novel activators of this recalcitrant target we opted to run a high-throughput screen (HTS).[18] The HTS was run using cAMP homogeneous time-resolved fluorescence (HTRF) kits from Cisbio. We found that for this target, cell lines overexpressing the hD1 receptor in an HEK cell background were more sensitive than those in a CHO cell background; we thus elected to screen in an HEK293 cell line.

To increase the probability of detecting weak or low partial agonists in an HTS format, we initially chose to analyze our functional response data in ratio mode relative to dopamine, using its signal as the 100% effect, as opposed to the more conventional analysis method employing a cAMP standard curve to convert the data to nM cAMP prior to normalizing to the dopamine control. Analyzing the data in ratio mode has the effect of enhancing a partial agonist's maximal

effect relative to dopamine which we theorized would help us identify compounds that would otherwise fail to be detected. For example, the known D1 partial agonist **3**[19] appears as a relatively full agonist when analyzed relative to dopamine, but as a partial agonist when analyzed using the cAMP standard curve (Figure 2A). This analysis was only used to triage HTS hits. Once SAR efforts commenced in earnest, we switched to using a conventional cAMP standard curve analysis of the data (cAMP mode, Table 1).

Using this approach, we queried approximately 3 million compounds in the Pfizer screening file in a compressed format (multiple compounds per well) in the presence of an EC_{10} of dopamine, so as to capture both PAMs and agonists. In this way, 1,200 compounds with ≥30% maximal response relative to dopamine were identified (Figure 2B). Catechol- and phenol-containing compounds, ergot alkaloid derivatives,[20] and compounds with either D2 preference (>10-fold D2/D1) or a strong response in a non-D1-overexpressing parental HEK293-cell line were eliminated. A final round of confirmatory screening using samples prepared from solid material with confirmed purity yielded only one hit, compound **6,** which exhibited an EC_{50} of approximately 1 μM and an 83% maximal response relative to dopamine. It is instructive to note that had we used the cAMP standard curve to analyze the screening data, we might have missed this hit, as it gave only borderline potency and efficacy values (~2.5 μM and 34%, respectively; Figure 2C).

In addition to elevation of cAMP in the HEK cell line, in an orthogonal readout of target engagement, compound **6** displayed direct binding to the human D1 (hD1) receptor in a radioligand displacement assay utilizing [^{3}H]SCH-23390[21] K_i = 2.2 μM). This data suggested that compound **6** binds in or near the orthosteric site. Compound **6** does not share structural similarity with known pan-assay interference compounds (PAINs)[22] and was not promiscuous in a focused pharmacology panel comprising GPCRs (9 targets, agonist and antagonist functional

endpoints, >10 μM), ion channels (4 targets, >10 μM) and phosphodiesterases (11 targets, >100 μM).

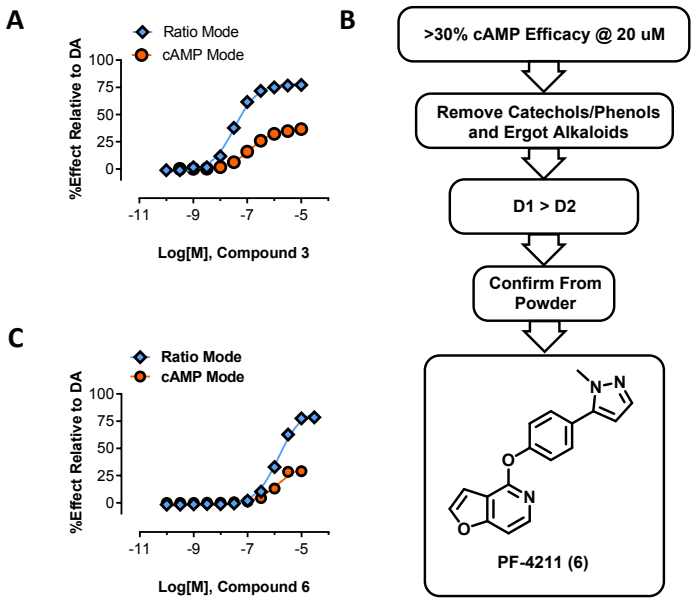

Figure 2: A) Composite cAMP functional dose-response curve of D1 partial agonist compound **3** (N=≥50) in an HEK cell line overexpressing hD1R. Data plotted according to 2 different analysis methods: ratio mode (blue) and cAMP mode (red); B) High-level D1 HTS screening funnel. Compound **6** was the sole confirmed hit from this screening campaign; C) Composite cAMP functional dose-response curve in ratio mode (EC_{50}: 1.0 μM, 83% maximal effect) and cAMP mode (EC_{50}: ~2.5 μM, 34% maximal effect) of D1 HTS hit compound **6** (N=≥40) in the absence of exogenous dopamine in an HEK293 cell line overexpressing the hD1 receptor.

Synthesis: The modular structure of compound **6** was exploited to rapidly generate SAR around the A, B and C ring systems (Figure 3) entirely by parallel medicinal chemistry (PMC).[15] Early work targeting ether linker replacements was non-productive, leading us to theorize that the ether function between rings B and C provides a desirable orientation for D1 binding, in which the pyridine lone pair repels the oxygen lone pairs, creating an orientation biased as drawn (Figure 3).[23] The A-B linkage was established through coupling reactions of available monomers, using standard palladium-catalyzed Suzuki cross-coupling, or via condensation

reactions to assemble the A ring heterocycles. S_NAr coupling reactions delivered the B-C ether bond through use of the commercial chlorofuropyridine **7**.

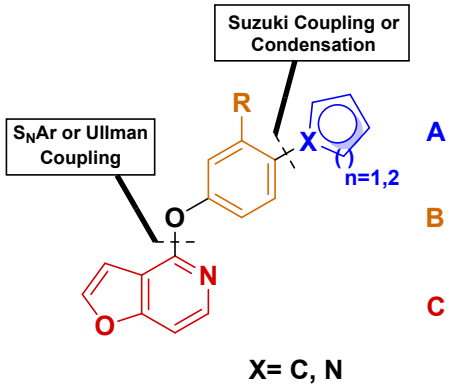

Figure 3: Key synthetic disconnections for analogs of compound **6**. Highlighted: heterocyclic **A** ring (blue), phenyl core **B** ring (orange), furopyridine **C** ring (red).

Pyrazole-containing analogs with diversity introduced at the 1-nitrogen of the pyrazole were prepared as shown in Route A (Scheme 1). Synthesis of these derivatives proceeded via S_NAr reaction between chlorofuropyridine **7** and the requisite phenolic acetophenone. Subsequent treatment of **8a,b** with DMF-DMA provided PMC templates **9a,b**, which were then condensed with substituted hydrazines in a parallel format to give substituted pyrazoles **18**–**20**. Pyrazole **6** was prepared in an analogous fashion, as shown in Route C, via an Ullman coupling of **7** with intermediate **13**.

Heterocyclic diversity on the A ring was primarily achieved using Route B. Aryl bromide templates **10a** and **10b** were prepared by S_NAr reaction of **7** with 4-bromophenol and 4-bromo-3-methylphenol, respectively. Subsequent Suzuki cross-coupling of **10b** with the appropriate heterocyclic boronate provided compound **17**. An orthogonal approach involved synthesis of boronate templates **11a,b** via treatment of bromides **10a,b** with bis(pinacolato)diboron under

palladium catalysis. Heterocyclic halides[24] were coupled with **11a,b** under palladium-catalyzed cross-coupling conditions to provide analogs **23–29.**

N-Linked azabenzimidazoles at the A ring were constructed as shown using route D: 4-chloro-3-nitropyridine (**15**) underwent S_NAr displacement with commercial anilines **14a,b** to provide biaryl intermediates. Reduction of the nitro functional group via hydrogenation, followed by condensation with ethyl orthoacetate, afforded the corresponding *N*-aryl azabenzimidazoles. Demethylation of the methyl ether with BBr_3 provided phenols **16a,b**, which were coupled under Ullmann conditions with chlorofuropyridine **7** to provide compounds **21** and **22**.

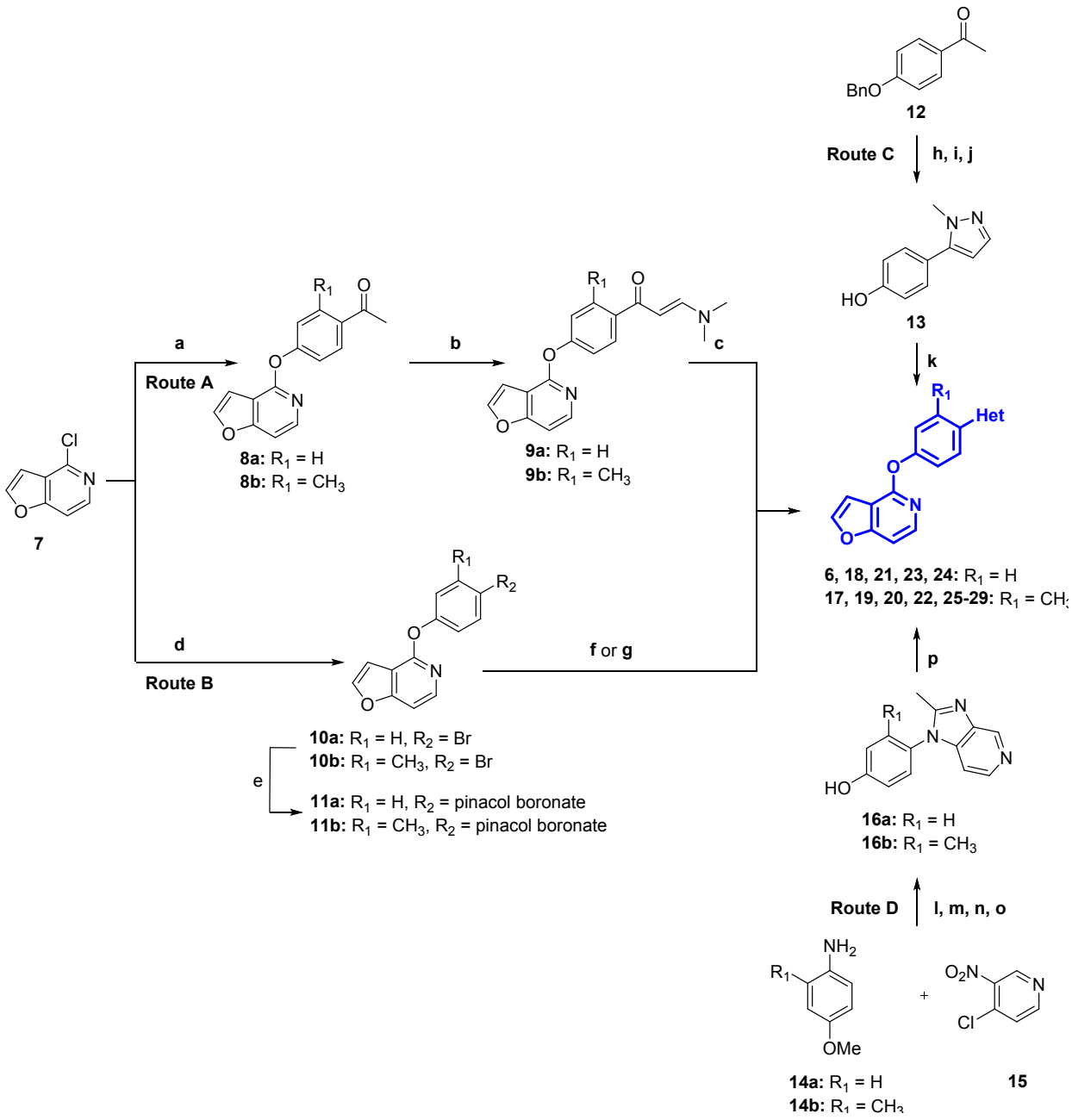

Scheme 1: (a) 1-(4-hydroxyphenyl)ethan-1-one or 1-(4-hydroxy-2-methylphenyl)ethan-1-one, Cs_2CO_3, CsF, NMP, 120 °C, 72 h; (b) DMF-DMA, DMF, Et_2O-BF_3, 110 °C, 6 h; (c) *t*-butylhydrazine HCl, MeOH, H_2O, HCl, 30 °C, 16 h; (d) 4-bromophenol or 4-bromo-3-methylphenol, Cs_2CO_3, DMSO, 125 °C, 16 h; (e) bis(pinacolato)diboron, Pd(dppf)Cl_2, KOAc, 85 °C to 100 °C, 16 h; (f) compound **10a** or **10b**, heteroaryl boronic acid, Na_2CO_3, $Pd(PPh_3)_4$, dioxane, H_2O, 130 °C, 1 h, microwave; (g) compound **11a** or **11b**, heteroaryl bromide, $Pd(OAc)_2$ or $Pd(PPh_3)_4$, K_2CO_3, DMF/H_2O, 70 °C to 80 °C, 0.5–18 h; (h) DMF-DMA, reflux, 16 h; (i) methylhydrazine, 75 °C, 3 h; (j) 1 atm

H_2, Pd/C in EtOH, H_2O, rt, 16 h; (k) compound **7**, Cs_2CO_3, CuI, 2,2,6,6-tetramethyl-3,5-heptanedione, NMP, 130 °C, 16 h; (l) Et_3N, EtOH, 16 h; (m) 45 psi H_2, Pd/C, MeOH, 24 h; (n) Ac_2O, $CH_3C(OEt)_3$, 145 °C, 1 h then 100 °C, 48 h; (o) BBr_3, CH_2Cl_2, −78 °C to rt; (p) compound **7**, Cs_2CO_3, DMSO, 140 °C, 16 h.

SAR Studies: In the initial rounds of PMC, monomer diversity was prioritized over the physical chemical properties of the final analogues in order to maximize diversity and increase the probability of identifying potency trends. Final compounds were limited to those with a cLogP < 6.5 and molecular weight <450. Varying the A and C rings using established chemistry furnished nearly 1,000 compounds in this initial design cycle. For brevity, only compounds whose SAR guided the discovery of compound **29**[25] are showcased (Table 1).

Preliminary SAR around the pyrazole tail group was generated using condensation chemistry (Scheme 1, Route A). This library yielded compounds **17**–**20**, which were more potent activators of D1 than HTS hit **6** and also had increased affinity in the binding assay. The greatest impact of this data was the observation that increasing steric bulk about the biaryl bond imparted significant gains in both D1 affinity and functional activity, leading to the structural hypothesis that orthogonal presentation of the A and B rings (Figure 4) results in improved receptor interactions. These gains in activity were also realized with the matched molecular pair (MMP)[26] imidazopyridines **21** and **22** which were derived using Route D. This pair, featuring di- and tri ortho-substituted biaryl bonds, showed only a modest increase in functional potency and binding affinity, 0.3 and 2-fold respectively relative to each other indicating limits to the activity gains that can be acheived using this strategy.

Methoxyisoquinoline **23** and imidazopyridine **24** were notable because they were the first compounds synthesized in this chemical series with a binding affinity K_i < 100 nM. The mono ortho-substituted biaryl system of compound **24** provided an opportunity to use the knowledge gained from the preliminary SAR generated on the pyrazoles to prospectively design for

increased potency, by increasing the energy required for the biaryl bond to rotate, as depicted in Figure 4.

Replacing the phenyl core with an *ortho*-tolyl ring (**25**) gave a 3-fold boost in potency and affinity over its MMP compound **24**. Adding a methyl on the imidazopyridine tail group, affording compound **26**, provided impressive gains in potency and affinity, 7-fold and 12-fold respectively, versus MMP compound **24**. Combining the methyl imidazopyridine tail group with the toluene core gave compound **27**, which exhibited no gain in affinity relative to compound **26** but was functionally 2-fold more potent. Importantly, compound **27** demonstrated a functional EC_{50} < 100 nM in the recombinant cell system; its cLogP (5.1), however, was outside of our targeted range. Triazolopyridine **28**, which offers lower lipophilicity, lost considerable potency and affinity relative to its MMP triazolopyridine **25**. This can be partially attributed to a significantly reduced torsional barrier (7.1 vs 12.4 kcal/mol). The potency and affinity of imidazopyridine **29**, however, was similar to compound **27**, while providing a 1.1 unit decrease in cLogP.

The LipE[27] analysis (Figure 5) of the compounds in Table 1 summarizes the improvement in chemical matter made from HTS hit **6** (binding LipE: 2.1) over the three described design cycles that ultimately culminated in compound **29** (binding LipE 4.1). The first design cycle, using PMC to target replacements of the A ring, provided **24**, whose increased activity was offset by increased lipophilicity resulting in a marginal improvement in LipE (binding LipE Δ: +0.2). The second design cycle sought to improve potency by increasing the torsional barrier about the biaryl bond between the A and B rings, resulting in the design and synthesis of compound **27**. Despite the increase in lipophilicity of **27**, the additional potency and affinity netted nearly a full unit increase in LipE (binding LipE Δ: +0.8). In the third design cycle, efforts to decrease lipophilicity by incorporating additional heteroatoms into the A ring

were rewarded by discovery of imidazopyridine **29**, which retained similar D1 potency and affinity to **27**, thus affording a full unit improvement in LipE.

Table 1: SAR

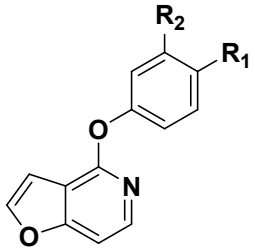

Cmpd #	R_1	R_2	D1 EC_{50} (nM), % Effect[a]	D1 hK_i[b] (nM)	LipE[c] Functional	LipE[c] Binding	ΔE[d] (kcal/mol)
1	N/A	N/A	232, 100%	243	6.2	6.4	N/A
6	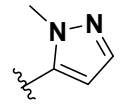	H	2,293, 37%	2,242	2.1	2.1	2.1
17	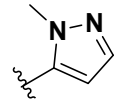	Me	1,232, 34%[e]	254	2.2	2.9	5.7
18	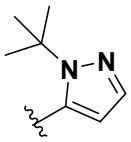	H	2,411, 11%[e]	1,680[e]	0.9	1.0	0.3
19	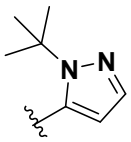	Me	1,108, 7%[e]	563[f]	1.0	1.3	11.1
20	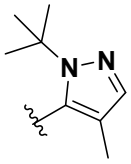	Me	895, 18%[e]	121[f]	1.1	2.0	16.2

21	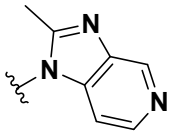	H	1,141, 73%	376	1.9	2.3	6.7
22	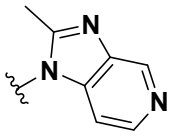	Me (Racemic)	416, 82%	244	1.5	2.1	14.5
23	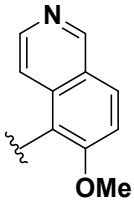	H	1,333, 64%	56.3	1.3	2.6	9.9
24	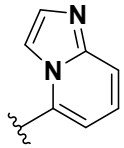	H	821, 61%	98.9	1.4	2.3	4.8
25	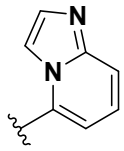	Me	262, 54%	38.1	1.7	2.6	12.4
26	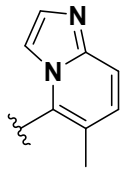	H	123, 62%	8.5	1.9	3.2	10.6
27	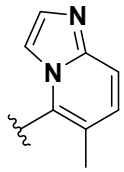	Me (Racemic)	64, 64%	6.8	2.1	3.1	17.2
28	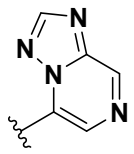	Me	5,485, 26%	2,346	2.6	2.8	7.1
29	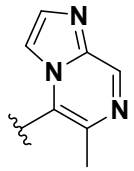	Me (Racemic)	106, 86%	8.9	3.0	4.1	17.4

30	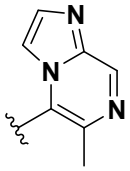	Me (R-enantiomer)	141, 89%	21.6	2.9	3.7	17.4
31	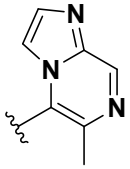	Me (S-enantiomer)	33, 91%	11.9	3.4	4.0	17.4

[a]Functional potency (EC_{50}) and intrinsic activity (eMax) as a % relative to the maximal effect of dopamine in HEK293T cells overexpressing the human D1 receptor (geometric mean; N ≥ 3 unless otherwise specified); Data was converted to nM cAMP prior to normalization to dopamine control; [b]Radioligand binding (geometric mean; N ≥ 3 unless otherwise specified); [c]Lipophilic efficiency (LipE) defined as D1 functional pEC_{50} or binding pK_i – cLogP; [d]Torsion scan calculations were performed by rotating around the bond connecting the two rings in the biaryl motif over a range of −180 to +180 degree in 15 degree angle increments using DFT(B3LYP)/6-31G**//6-31G** from a TeraChem software package; [e]N = 1; [f]N = 2; N/A = not applicable.

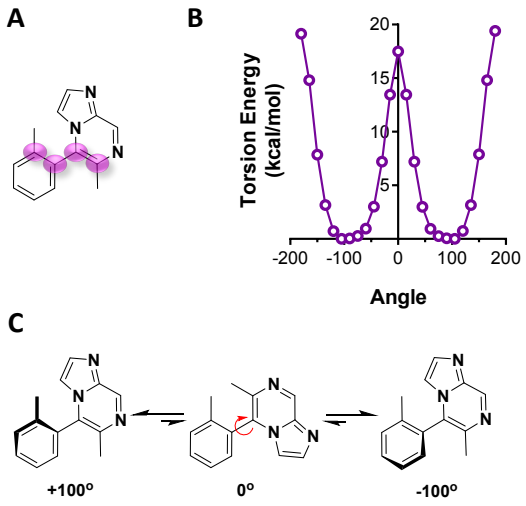

Figure 4: (A) Highlighted atoms about the biaryl bond indicate the torsion motif used for the dihedral scan measurement; (B) Rotational energy barrier and example QM torsion plot of compound **29** over a range of −180 to +180 degrees in 15 degree angle increments using DFT(B3LYP)/6-31G**//6-31G** from a TeraChem software package; (C) Defined torsional angles.

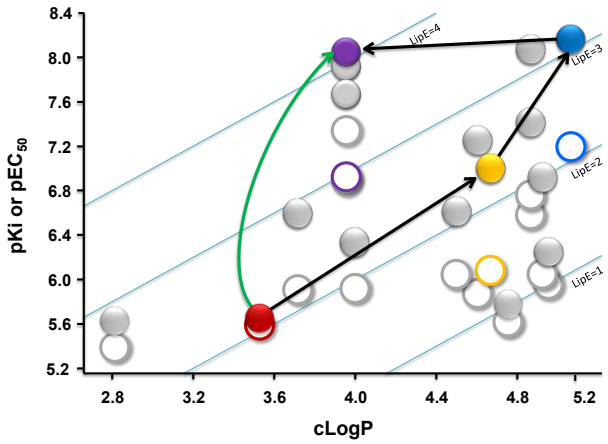

Figure 5: LipE plot of cLogP (X-axis) vs D1 activity (Y-axis). Open circles are the D1 agonist functional activity pEC_{50}; Solid circles are the D1 binding pK_i. Red is compound **6**; Yellow is compound **24**; Blue is compound **27**; Purple is compound **29**; All other compounds are grey. Black arrows indicate the progress made over three design cycles, while the green arrow is the progress made from the initial D1 HTS hit compound **6** to compound **29**.

Atropisomerism: The physical consequence of increasing the barrier to rotation between two rings is atropisomerism.[28] In our experience, a biaryl bond with a calculated energy barrier to rotation of >15 kcal/mol (Table 1, Figure 4) is likely to provide two stable chiral atropisomers at physiologically relevant temperatures[29]. The individual atropo-enantiomers of compound **29**, compounds **30** and **31,** were separated by chiral supercritical fluid chromatography (SFC)[30] and tested in our primary pharmacology assays. Enantiomer **31** had a 4-fold higher potency and 2-fold higher affinity towards D1 than its mirror image **30**.

An analytical sample of **31** was heated to 37 ^{o}C in 2-butanol for 72h and checked for racemization. No racemization was detected by HPLC analysis indicating that the thermal barrier to interconversion is high enough to have physiological relevance**.** The absolute stereochemistry of atropo-enantiomer **31** was determined to be aS/P (depending on the nomenclature)[31] by light atom X-ray crystallography using the Hooft method.[32] This assignment was further supported by

independent assignment of the less active enantiomer as aR/M **30** using the orthogonal vibrational circular dichroism (VCD) spectroscopy method.[33]

Understanding that the energetics of atropisomer interconversion would be relevant for both synthetic chemistry and any therapeutic advancement for compounds in this hindered biaryl bond series, we used a streamlined segmented flow method[34] to experimentally determine accurate $\Delta G^{\ddagger}$ and $T_{1/2}$ values for racemization of compound **30** in solvents of interest (Figure 6; see SI for data). For example, using this approach, we determined these parameters for **31** and chiral intermediates leading to **31** (Figure 6B). Route development efforts for compound **31** were facilitated by the discovery that these compounds can be resolved early in the synthesis and then handled in the laboratory for short periods of time, even at temperatures up to 100 °C in solution (extrapolated $T_{1/2}$ = 18 days), without risk of significant erosion of enantiopurity.

A

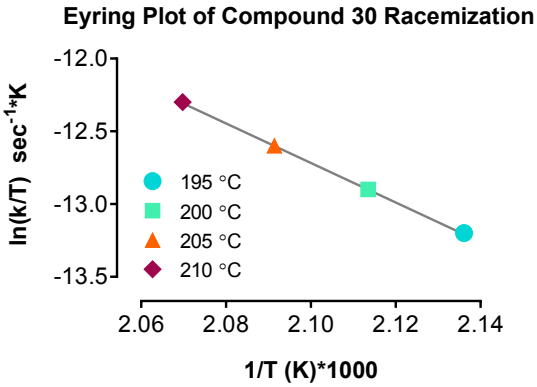

B

Measured Activation Parameters

ΔH‡	ΔS‡	units
26.8	-0.01621	kcal/mol & kcal/mol•K

C **Extrapolations from Y = -13489X + 15.604**

T (°C)	ΔG kcal/mol	$T_{1/2}$	units
0	31.2	37620	years
25	31.6	548	years
37	31.8	91.6	years
60	32.2	4.2	years
100	32.9	18.0	days
250	35.4	35	seconds

Figure 6: (A) Eyring plot for the racemization of compound **30** in a 3-methylbutan-1-ol/toluene (97:3) solution; (B) Calculated activation parameters for compound **30**; (C) Extrapolated ΔG‡ and $T_{1/2}$ at temperatures ranging from 0–250 °C.

While our in vitro kinetics study predicted an acceptable half-life for potential development of **31** as a single atropo-enantiomer, the presence of serum proteins in vivo can affect the rate of interconversion;[35] thus, an in vitro study was conducted to determine the rate of interconversion under conditions simulating an in vivo system, by incubating compounds **29**–**31** in human blood, human plasma, and human serum albumin at 37 °C for 24 h followed by quantitative analysis. In all matrices tested, there was no evidence of interconversion.

Physical Chemical Properties and Pharmacokinetics: With the exception of moderately high lipophilicity (cLogP and measured ElogD[36]) (Table 2), compound **31** has well-aligned physical chemical properties (EPSA,[37] pK_a, and lack of HBD) for CNS penetration (CNS MPO[38]: 4.9). Low MDR and BCRP efflux ratios,[39] high cell permeability, and low turnover by human liver microsomes (HLM) contribute to its favorable profile. In rat, compound **31** had excellent brain availability ($C_{b,u}/C_{p,u}$ = 0.8, good IV clearance and half-life, and high oral-bioavailability.

Table 2: Summary of calculated and measured chemical properties, ADME, and rat in vivo PK for compound **31**

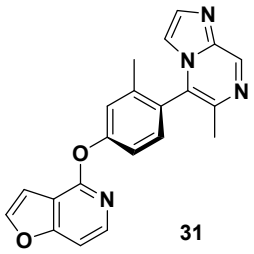

31

Chemical Properties	In vitro ADME
MW: 356.4 ElogD/cLogP: 3.4/4.0 EPSA: 57 Melting pt: 142-144 °C Aq.sol., pH 7.4: 132 μM[a] pK_a: 4.1	MDR: 1.7[b] BCRP: 1.3[c] RRCK: 31 x 10^{-6} cm/sec[d] HLM: 22 mL/min/kg[e]
Protein Binding[f]	**Rat In vivo PK**
human $F_{u,p}$: 0.04 rat $F_{u,p}$: 0.04 mouse $F_{u,p}$: 0.04 rat $F_{u,b}$: 0.02	B/P[g] = 2.2 $C_{b,u}/C_{p,u}$[h] = 0.8 $T_{1/2}$ = 2.3 h Cl = 23 mL/min/kg[i] F% = 85%[j]

[a]Measured thermodynamic solubility of crystalline solid. [b]Ratio of permeability measured as a rate in 10^{-6} cm/s in and out (BA/AB) of a Madin-Darby canine kidney (MDCK) epithelial cell line transfected with the MDR1 gene encoding the P-gp efflux transporter. [c]Ratio of permeability measured as a rate in 10^{-6} cm/s in and out (BA/AB) of a BCRP-transfected MDCK cell line.[40] [d]Permeability in the MDCKII-LE (RRCK)[40] cell line, given as a rate in 10^{-6} cm/s. [e]Intrinsic clearance in human liver microsomes (HLM). [f]Fraction unbound[41] in plasma ($F_{u,p}$) or brain ($F_{u,b}$). [g]AUC ratio of the drug level in rat brain to the drug level in plasma. [h]AUC ratio of the unbound drug level in rat brain to the unbound drug level in plasma from a single subcutaneous dose of 5.6 mg/kg. [i]Observed blood clearance in units of mL/min/kg following a single IV bolus of 5.0 mg/kg, dosed as a solution in saline containing 3 molar equivalents of HCl. [j]Oral bioavailability following 5 mg/kg dosed PO in a 0.5% methylcellulose vehicle.

Biology and Pharmacology: Compound **29** and its atropo-enantiomer **31** were invaluable tool compounds to strengthen our confidence that, despite the lack of structural similarity to known D1 agonist ligands, this chemical series exerts its pharmacology at the D1 receptor both *in-vitro* and *in-vivo*. Compound **31** was submitted to a broad panel of targets to assess its promiscuity. The panel consisted of agonist and antagonist functional readouts of 9 GPCR's, 5 ion channels, 3 transporters, and 11 phosphodiesterases (PDEs). Compound **31** exhibited IC_{50}'s <5 μM as an antagonist at the following 4 targets: M_1: 4.9 μM, CB1: 2.1 μM, H_1: 4.6 μM, and Nav 1.5: 1.1 μM. It has a hERG IC_{50} of approximately 12 μM. It is important to reiterate that D1 shares considerable homology with D5 and that none of the currently available agonists distinguish between D1 and D5; this includes **31** which has a D5 Ki of 4.8 nM. It is, however, exquisitely selective vs D2 (Ki >10 μM).

Agonist activation of D1-like receptors (D1R), which include the D1 and D5 subtypes, has been previously reported to increase locomotor activity in mice[42] via a cAMP-dependent mechanism. Therefore, the ability of D1 agonist compounds of interest to increase locomotor activity in mice was used to confirm in vivo functional activity. Compound **29** was tested in the habituated mouse locomotor assay at multiple test doses (Figure 7A). Similar to other D1

agonists, treatment with compound **29**, at the 10 and 32 mg/kg doses produced significant increases in locomotor activity during the 0-120 minute post-dose time period as compared to vehicle treatment (Figure 7A). The specificity of this activity was verified when pre-treatment with D1 antagonist SCH-23390[43] (**32**) attenuated the increase in a dose-dependent manner (Figure 7B).

Cultured rat primary striatal neurons endogenously expressing D1[44] were used to assess compound-driven D1 desensitization. Cells were incubated with 10 μM of D1 agonists **1–4**, A77636 (**33**)[45], and SKF-83959 (**34**)[46] for 90 min, thoroughly washed, and then challenged with D1 catecholamine agonist **4** to measure cAMP response. Figure 7C shows that the D1 catecholamine agonist group (**1–4**, **33** and **34**) induced significant levels of D1 desensitization (~60-100%), whereas the D1 non-catecholamine agonist group (**29**–**31**) had a significantly reduced degree of desensitization (~20%). The vehicle-pretreated group was normalized to 0% desensitization. This result suggests that, compared to the catecholamines, the non-catecholamine agonists are biased towards less desensitization in an endogenous D1 cell system. Further, we have previously published that, in-vivo, a compound with less β-arrestin recruitment relative to **33** has a sustained in-vivo response, even after repeated dosing, in a cynomolgus monkey eye blink rate study.[15]

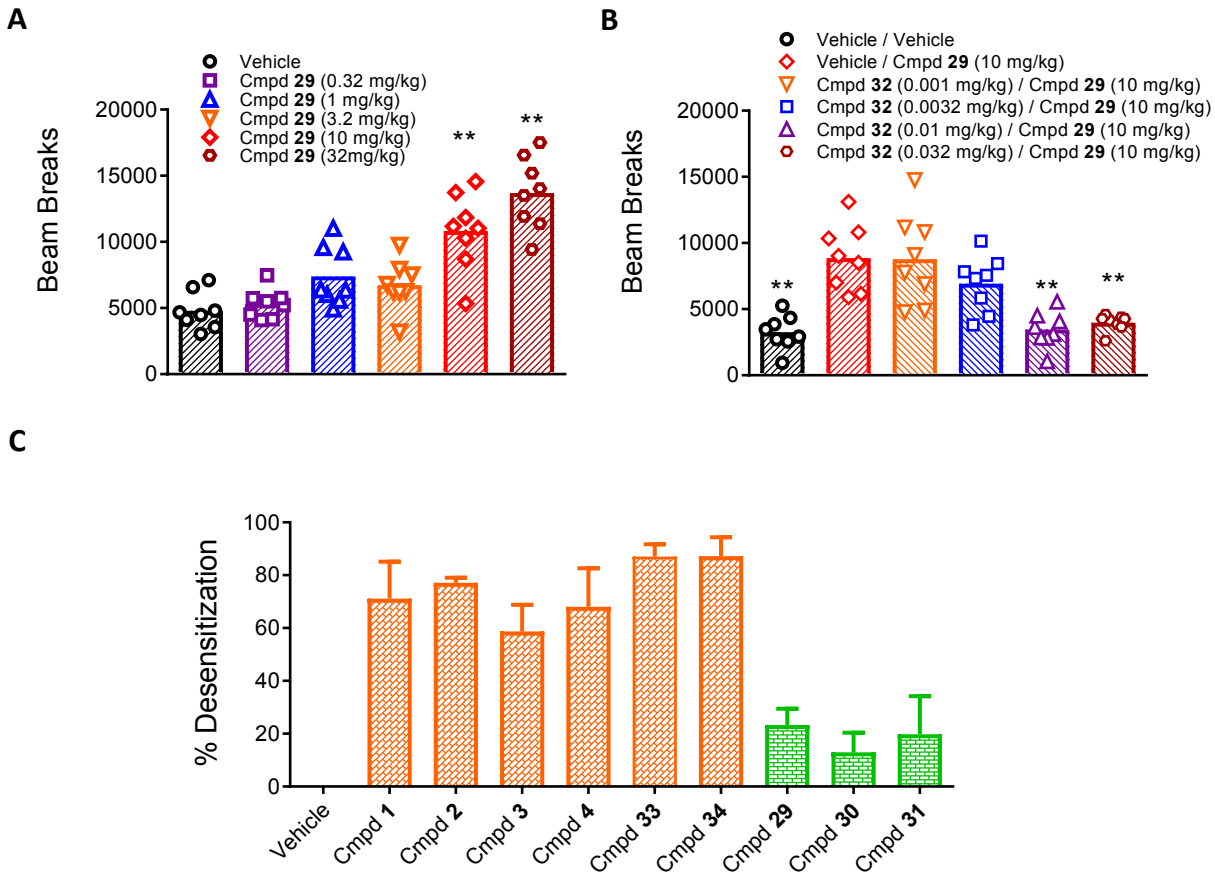

Figure 7: Locomotor activity (total beam breaks during 2 hours) in response to administration of D1 agonists/antagonists. (A) Treatment with compound **29**, at 10 and 32 mg/kg, SC, increases the number of beam breaks. (B) Pretreatment with the D1 antagonist, compound **32**, dose-dependently blocks the hyperactivity induced by compound **29** at 10 mg/kg, SC. One-sided ANOVA with Dunnett's post-test adjusted ** $p < 0.05$, ** $p < 0.01$ vs vehicle or vs vehicle plus compound **29** (10 mg/kg). (C) Desensitization by catechol agonists (orange) **1**-**4**, **33** and **34** versus non-catechol agonist compounds **29**–**31** (green) using a cAMP readout, towards subsequent challenge with agonist SKF-81297.[46]

Conclusions

Herein we describe the discovery and optimization of the first D1-selective agonist chemical series with suitable physicochemical properties for oral absorption, brain exposure, and low clearance. These compounds represent a significant step forward for the exploration of D1

activation. Extensive SAR generated on the A and B rings by PMC quickly provided compounds with increased potency and binding affinity for the D1 receptor, as well as an early observation that conformationally restraining these rings into an orthogonal relationship provides a consistent potency and binding affinity benefit; this led to the discovery of compound **29**. Separation of compound **29** into its atropisomers provided the more active enantiomer **31**. Compound **31** has excellent D1 potency and is selective against D2 and other GPCRs, ion channels, and PDEs.

The pharmacokinetic properties of **29**/**31** such as metabolic stability, high passive permeability and low MDR and BCRP efflux ratios, make this compound suitable for oral dosing and in vivo study. In vitro pharmacology experiments with **29**–**31** revealed an intriguing D1 receptor desensitization profile relative to catechol-containing D1 agonists including dopamine. This pharmacological profile merits clinical study because in chronic diseases, such as schizophrenia and Parkinson's disease, the duration of therapeutic effect is an important component of patient quality of life.

Experimental:

All procedures performed on animals in this study were in accordance with established guidelines and regulations, and were reviewed and approved by the Pfizer Institutional Animal Care and Use Committee. Pfizer animal care facilities that supported this work are fully accredited by AAALAC International.

Chemistry General Information. All solvents and reagents were obtained from commercial sources and were used as received. All reactions were monitored by TLC (TLC plates F254, Merck) or UPLC-MS analysis (Waters Acquity, ESCI +/−, APCI +/−). Melting points were obtained with a Thomas–Hoover melting point apparatus and are uncorrected. ^{1}H NMR spectra

were obtained using deuterated solvent on a Varian or Bruker 400 MHz instrument. All ^{1}H NMR shifts are reported in δ units (ppm) relative to the signals for chloroform (7.27 ppm), DMSO (2.50 ppm) and MeOH (3.31 ppm). All coupling constants (J values) are reported in hertz (Hz). NMR abbreviations are as follows: br, broadened; s, singlet; d, doublet; t, triplet; q, quartet; p, pentuplet; m, multiplet; dd, doublet of doublets; ddd, doublet of doublet of doublets. HPLC purity analysis of the final test compounds was carried out using one of three methods. Method A: UPLC/UV. WuXi AppTec, Shanghai, China. Column: Agilent Xtimate C18, 5 × 30 mm, 3 μm; UV purity detected at 220 nm; Mobile phase A = 0.1% TFA in H_2O; Mobile phase B = 0.1% TFA in CH_3CN. Gradient: 1% B to 100% B in 5.0 min. Flow rate: 1.2 mL/min. Method B: UPLC/UV WuXi AppTec, Shanghai, China. Column: XBridge C18, 2.1 × 50 mm, 5 μm; UV purity detected at 220 nm; Mobile phase A = 0.0375% TFA in H_2O; Mobile phase B = 0.01875% TFA in CH_3CN. Gradient: 1% B to 5% B in 0.6 min, 5% B to 100% B in 4.4 min, 100% B to 1% B for 0.3 min, hold at 1% B for 0.4 min. Flow rate: 0.8 mL/min. Method C: Column: Waters Atlantis C18, 4.6 x 50 mm, 5 μm; UV purity detected at 215 nm; Mobile phase A: 0.05% TFA in H_2O (v/v); Mobile phase B: 0.05% TFA in CH_3CN (v/v); Gradient: 5% B linear to 95% B in 4.0 min, hold at 95% B to 5.0 min. Flow rate: 2 mL/min. All final compounds were determined to have a purity of >95% by one of the aforementioned methods.

Experimental

4-(4-(1-Methyl-1H-pyrazol-5-yl)phenoxy)furo[3,2-c]pyridine (6). To a stirred solution of **13** (60 mg, 0.340 mmol) and 4-chlorofuro[3,2-*c*]pyridine (**7**) (106 mg, 0.688 mmol) in NMP (2 mL) were added cesium carbonate (283 mg, 0.860 mmol), copper(I)iodide (33 mg, 0.172 mmol), and 2,2,6,6-tetramethyl-3,5-heptanedione, and the reaction mixture was heated to 130 ºC for 16 h. After addition of water (30 mL), the layers were separated and the aq layer was extracted with

1:1 diethyl ether/hexanes (4 x 30 mL). The combined organic layers were dried over sodium sulfate, filtered, and concd *in vacuo*. Purification via silica gel chromatography (Gradient: 30% to 60% EtOAc in heptanes) afforded a white solid. The white solid was further purified by HPLC. Xbridge column, (TFA as modifier, 5% to 100% acetonitrile in water) to afford **6** as a white solid in 49% yield. ^{1}H NMR (400 MHz, CD_3OD) δ 7.96 (d, *J* = 6.1 Hz, 1H), 7.89 (d, *J* = 2.1 Hz, 1H), 7.56 (d, *J* = 8.6 Hz, 2H), 7.51 (d, *J* = 2.0 Hz, 1H), 7.37 (dd, *J* = 6.0, 0.9 Hz, 1H), 7.32 (d, *J* = 8.8 Hz, 2H), 6.93 (dd, *J* = 2.2, 0.9 Hz, 1H), 6.39 (d, *J* = 2.0 Hz, 1H), 3.91 (s, 3H). MS (ES^+): *m/z* 292.3 [M + 1].

1-(4-(Furo[3,2-c]pyridin-4-yloxy)phenyl)ethan-1-one (8a). A stirring mixture of 1-(4-hydroxyphenyl)ethan-1-one (4.9 g, 36 mmol), **7** (5.5 g, 36 mmol), cesium fluoride (5.5 g, 36 mmol), and cesium carbonate (11.7 g, 36 mmol) in NMP (50 mL) was heated at 120 ºC for 72 h. The reaction mixture was partitioned between water (150 mL) and EtOAc (300 mL); the organic layer was washed with 5% NaOH and water, dried over magnesium sulfate, and concd *in vacuo.* Purification by silica gel chromatography (Eluent: hexane/EtOAc, 10:1) afforded **8a** as an oil in 30% yield.

3-(Dimethylamino)-1-(4-(furo[3,2-c]pyridin-4-yloxy)phenyl)prop-2-en-1-one (9a). A stirring mixture of **8a** (5.8 g, 23 mmol) and DMF-DMA (7.74 g, 65 mmol) in DMF (20 mL) and several drops of boron trifluoride etherate was heated at 110 ºC for 6 h. After removal of solvent under reduced pressure, the residue was treated with EtOAc (200 mL) and washed with water (150 mL). The organic layer was separated, dried (sodium sulfate), and concd *in vacuo.* The residue was treated with diethyl ether (50 mL) and the resulting precipitate was filtered off, washed with hexane, and dried to provide **9a** as a yellow solid in 73% yield.

4-(4-Bromophenoxy)furo[3,2-c]pyridine (10a). To a solution of **7** (10 g, 65 mmol) in NMP (200 mL) were added cesium carbonate (65 g, 200 mmol) and 4-bromophenol (14.7 g, 91 mmol),

and the reaction was heated to 130 °C for 16 h. At this point, the reaction mixture was cooled to rt, poured into water (400 mL), and extracted with EtOAc (3 x 200 mL). The combined organic layer was dried over anhydrous sodium sulfate, filtered, and concd *in vacuo*. Purification by chromatography on silica gel (Eluent: petroleum ether) afforded **10a** as a pale yellow solid in 86% yield. ^{1}H NMR (400 MHz, $CDCl_3$) δ 8.01 (d, *J* = 5.9 Hz, 1H), 7.66 (d, *J* = 2.4 Hz, 1H), 7.54 (d, *J* = 8.6 Hz, 2H), 7.22 (d, *J* = 6.7 Hz, 1H), 7.13 (d, *J* = 8.6 Hz, 2H), 6.90 (d, *J* = 1.2 Hz, 1H). MS (ES+): *m/z* 291.9 [M + 1].

4-(4-Bromo-3-methylphenoxy)furo[3,2-c]pyridine (10b). To a stirred solution of **7** (120 g, 781 mmol) in DMSO (1.56 L) were added cesium carbonate (509 g, 1.56 mol) and 4-bromo-3-methylphenol (161 g, 861 mmol), and the reaction was heated to 125 °C for 16 h. At this point, the reaction mixture was cooled to rt, poured into water (5 L), and extracted with EtOAc (2 x 2.5 L). The combined organic extracts were washed with water (2.5 L), washed with saturated aq NaCl solution (2.5 L), dried over anhydrous sodium sulfate, filtered, and concd *in vacuo*. Purification by chromatography on silica gel (Eluent: 2% EtOAc in petroleum ether) afforded **10b** as a pale yellow solid in 86% yield. ^{1}H NMR (400 MHz, $CDCl_3$) δ 8.00 (d, *J* = 6.2 Hz, 1H), 7.64 (d, *J* = 2.1 Hz, 1H), 7.55 (d, *J* = 8.3 Hz, 1H), 7.20 (dd, *J* = 5.8, 0.8 Hz, 1H), 7.12 (d, *J* = 2.9 Hz, 1H), 6.93 (dd, *J* = 8.5, 2.7 Hz, 1H), 6.88 (dd, *J* = 2.5, 0.8 Hz, 1H), 2.41 (s, 3H) . MS (ES+): *m/z* 304.0, 306.0 [M + 1].

4-[4-(4,4,5,5-Tetramethyl-1,3,2-dioxaborolan-2-yl)phenoxy]furo[3,2-c]pyridine (11a). To a stirred solution of **10a** (14 g, 48.3 mmol) in 1,4-dioxane (150 ml) was added bis(pinacolato)diboron (14.7 g, 58.0 mmol), potassium acetate (14.2 g, 145 mmol), and [1,1′-bis(diphenylphosphino)ferrocene]dichloropalladium(II) (3.4 g, 4.83 mmol) and the reaction mixture was heated at 100 °C for 16 h. After cooling to rt, the reaction mixture was poured into water (400 mL) and EtOAc (150 mL). The aq layer was extracted with EtOAc (3 x 200 mL), and

the combined organic layer was washed with brine, dried over anhydrous sodium sulfate, filtered, and concd *in vacuo*. The residue was purified by silica gel chromatography (Eluent: petroleum ether/EtOAc 50:1 to 10:1) to provide **11a** as a white solid in 70% yield. ^{1}H NMR (400 MHz, $CDCl_3$) δ 8.02–8.01 (d, 1H), 7.89–7.87 (d, 2H), 7.62–7.61 (d 1H), 7.21–7.19 (m, 3H), 6.81–6.80 (m, 1H), 1.35 (s, 12H). MS (ES+): *m/z* 338.2 [M + 1].

4-[3-Methyl-4-(4,4,5,5-tetramethyl-1,3,2-dioxaborolan-2-yl)phenoxy]furo[3,2-c]pyridine (11b). To a stirred solution of **10b** (50.0 g, 164 mmol) in 1,4-dioxane (1.02 L) was added bis(pinacolato)diboron (41.76 g, 164.4 mmol), potassium acetate (64.6 g, 658 mmol) and [1,1'-bis(diphenylphosphino)ferrocene]dichloropalladium(II) (6.0 g, 8.2 mmol), and the reaction mixture was heated at 85 °C for 16 h. After cooling to rt, it was filtered through a pad of Celite, and the pad was washed with EtOAc. The combined filtrates were concd *in vacuo* and the residue was purified by silica gel chromatography (Eluent: 2% EtOAc in petroleum ether) to afford **11b** as a white solid in 70% yield. ^{1}H NMR (400 MHz, $CDCl_3$) δ 8.02 (d, J = 5.8 Hz, 1H), 7.84 (d, J = 7.5 Hz, 1H), 7.61 (d, J = 2.1 Hz, 1H), 7.19 (d, J = 5.8 Hz, 1H), 7.00 (m, 2H), 6.80 (m, 1H), 2.56 (s, 3H), 1.34 (s, 12H). MS (ES^+): *m/z* 352.2 [M + 1].

5-[4-(Benzyloxy)phenyl]-1-methyl-1*H*-pyrazole. To a stirred solution of compound **12** (15.32 g, 67.71 mmol) in DMF (30 mL) was added DMF-DMA (94%, 19.0 mL, 134 mmol) and the reaction mixture was heated at reflux for 18 h, whereupon the reflux condenser was replaced with a distillation head, and distillation was carried out until the temp of the distillate reached 140 ºC. The material in the reaction pot was cooled to rt, treated with methylhydrazine (98%, 7.4 mL, 136 mmol), and heated at 75 ºC for 3 h. The reaction mixture was cooled, diluted with EtOAc, washed four times with aq 5% NaCl solution, dried over magnesium sulfate, filtered, and concd *in vacuo*. Purification via silica gel chromatography (Gradient: 2% to 10% EtOAc in DCM) afforded 5-[4-(benzyloxy)phenyl]-1-methyl-1*H*-pyrazole as a light yellow solid in 77%

yield. ^{1}H NMR (400 MHz, DMSO-d_6) δ 7.49–7.32 (m, 8H), 7.12 (d, J = 8.6 Hz, 2H), 6.32 (d, J = 1.9 Hz, 1H), 5.17 (s, 2H), 3.81 (s, 3H). MS (ES+): *m/z* 265.1 [M + 1].

4-(1-Methyl-1H-pyrazol-5-yl)phenol (13). To a stirred solution of 5-[4-(benzyloxy)phenyl]-1-methyl-1*H*-pyrazole (13.49 g, 51.04 mmol) in EtOH (125 mL) was added 10% palladium on carbon (~50% in water, 1.46 g). The reaction mixture was hydrogenated at rt and 1 atm hydrogen for 16 h, then filtered and concd *in vacuo*. The residue was triturated with heptane to afford **13** as a colorless solid in 98% yield. ^{1}H NMR (400 MHz, DMSO-d_6) δ 9.73 (br s, 1H), 7.40 (d, J = 1.9 Hz, 1H), 7.31 (br d, J = 8.7 Hz, 2H), 6.86 (br d, J = 8.7 Hz, 2H), 6.26 (d, J = 1.9 Hz, 1H), 3.79 (s, 3H). MS (ES+): *m/z* 175.1 [M + 1].

N-(4-Methoxy-2-methylphenyl)-3-nitropyridin-4-amine. A solution of 4-methoxy-2-methylaniline (**14b**) (23.8 g, 173 mmol), 4-chloro-3-nitropyridine (**15**) (25 g, 160 mmol), and triethylamine (33.0 mL, 237 mmol) in EtOH (250 mL) was stirred at rt for 16 h, then concd under reduced pressure. The residue was dissolved in EtOAc (200 mL) and filtered through a thick pad of silica gel (Eluent: EtOAc, 1 L). The filtrate was concd *in vacuo* to afford the title compound as a purple oil, which solidified on standing in 100% yield. This material was used without further purification. MS (ES$^+$): *m/z* 260.1 [M + 1].

N^4-(4-Methoxy-2-methylphenyl)pyridine-3,4-diamine. Palladium on carbon (10%, 3 x 2.12 g) was added to each of three batches of N-(4-methoxy-2-methylphenyl)-3-nitropyridin-4-amine (each approximately 10 g; total 31 g, 120 mmol) in MeOH (3 x 100 mL). The three suspensions were independently hydrogenated under 45 psi hydrogen at rt on a Parr shaker for 24 h. The three reaction mixtures were combined, filtered through a pad of Celite, and concd *in vacuo*. Purification by silica gel chromatography [Gradient: 2% to 10% (1.7 M ammonia in MeOH) in DCM] afforded the title compound as a light brown solid in 88% yield. ^{1}H NMR (400 MHz, $CDCl_3$) δ 8.01 (s, 1H), 7.88 (d, J = 5.5 Hz, 1H), 7.08 (d, J = 8.6 Hz, 1H), 6.84 (br d, J = 2.8 Hz,

1H), 6.78 (br dd, *J* = 8.6, 3.0 Hz, 1H), 6.34 (d, *J* = 5.5 Hz, 1H), 5.66 (br s, 1H), 3.82 (s, 3H), 2.20 (br s, 3H). MS (ES^+): *m/z* 230.1 [M + 1].

1-(4-Methoxy-2-methylphenyl)-2-methyl-1H-imidazo[4,5-c]pyridine. A stirred mixture of N^4-(4-methoxy-2-methylphenyl)pyridine-3,4-diamine (3.95 g, 17.2 mmol), acetic anhydride (1.96 mL, 20.7 mmol), and triethyl orthoacetate (99%, 15.9 mL, 86.4 mmol) was heated at 145 ºC for 1 h, then at 100 ºC for 48 h. After being cooled to rt, the reaction mixture was diluted with EtOAc (100 mL), washed with saturated aq sodium bicarbonate solution (30 mL), washed with water, dried over sodium sulfate, filtered, and concd under reduced pressure. Purification by silica gel chromatography (Gradient: 2% to 5% MeOH in DCM) afforded the title compound as a light pink oil in 94% yield. ^1H NMR (400 MHz, $CDCl_3$) δ 9.07 (br d, *J* = 0.8 Hz, 1H), 8.36 (d, *J* = 5.5 Hz, 1H), 7.15 (d, *J* = 8.6 Hz, 1H), 6.97–6.89 (m, 3H), 3.90 (s, 3H), 2.42 (s, 3H), 1.94 (br s, 3H). MS (ES^+): *m/z* 254.1 [M + 1].

3-Methyl-4-(2-methyl-1H-imidazo[4,5-c]pyridin-1-yl)phenol (16b). Boron tribromide (1 M solution in DCM, 44.1 mL, 44.1 mmol) was added drop-wise to a solution of 1-(4-methoxy-2-methylphenyl)-2-methyl-1*H*-imidazo[4,5-*c*]pyridine (3.72 g, 14.7 mmol) in DCM (150 mL) at −78 ºC. The reaction mixture was stirred at −78 ºC for 15 min, then the cooling bath was removed and the reaction mixture was allowed to gradually warm to rt. After 20 h at rt, the reaction mixture was re-cooled to −78 ºC and slowly quenched with MeOH (20 mL). At this point, the cooling bath was removed; the mixture was allowed to reach rt and then stir for 15 min. Volatiles were removed *in vacuo*, MeOH (100 mL) was added, and the mixture was heated at reflux for 30 min. After concentration under reduced pressure, the resulting solid **16b** was taken directly to the next step. MS (ES^+): *m/z* 240.1 [M + 1].

4-(3-Methyl-4-(1-methyl-1H-pyrazol-5-yl)phenoxy)furo[3,2-c]pyridine (17). A stirred mixture of **10b** (200 mg, 0.658 mmol), 1-methyl-1*H*-pyrazol-5-ylboronic acid (100 mg, 0.794

mmol), sodium carbonate (141 mg, 1.32 mmol), and tetrakis(triphenylphosphine)palladium(0) (80 mg, 0.066 mmol) in dioxane/water (13:3, 4 mL) was heated in a microwave at 130 ºC for 1 h. The reaction mixture was cooled, filtered through a Celite pad, and concd *in vacuo*. Purification via silica gel chromatography afforded **17** as an off-white solid in 44% yield. ^{1}H NMR (400 MHz, CD_3OD) δ 7.93 (d, *J* = 5.9 Hz, 1H), 7.85 (d, *J* = 2.3 Hz, 1H), 7.53 (br s, 1H), 7.34 (d, *J* = 5.9 Hz, 1H), 7.27 (d, *J* = 8.2 Hz, 1H), 7.16 (d, *J* = 2.0 Hz, 1H), 7.08 (dd, *J* = 8.3, 2.2 Hz, 1H), 6.89 (s, 1H), 6.26 (d, *J* = 1.4 Hz, 1H), 3.67 (br s, 3H), 2.14 (s, 3H). MS (ES^+): 306.1 [M + 1].

4-(4-(1-(*tert*-Butyl)-1H-pyrazol-5-yl)phenoxy)furo[3,2-c]pyridine (18). In library format, a solution of **9a** (75 μmol, 1 eq) and *tert*-butylhydrazine hydrochloride (90 μmol, 2 eq) in MeOH (750 μL) and 2M aq HCl (75 μL, 2 eq) were shaken at 30 ºC for 16 h. Solvents were removed *in vacuo* and the residue was purified by preparative HPLC to afford **18** as a white solid in 52% yield. ^{1}H NMR (400 MHz, $CDCl_3$) δ 8.07 (d, *J* = 5.9 Hz, 1H), 7.68 (d, *J* = 2.4 Hz, 1H), 7.51 (d, *J* = 1.6 Hz, 1H), 7.41 (d, *J* = 8.6 Hz, 2H), 7.32–7.22 (m, 3H), 6.92 (d, *J* = 1.6 Hz, 1H), 6.21 (d, *J* = 1.6 Hz, 1H), 1.53 (s, 9H). MS (ES^+): *m/z* 334.4 [M + 1].

4-(4-(1-(*tert*-Butyl)-1H-pyrazol-5-yl)-3-methylphenoxy)furo[3,2-c]pyridine (19). The title compound was prepared using methods closely related to those exemplified for **18**. MS (ES^+): *m/z* 348.0 [M + 1].

4-(4-(1-(*tert*-Butyl)-4-methyl-1H-pyrazol-5-yl)-3-methylphenoxy)furo[3,2-c]pyridine (20). The title compound was prepared using methods closely related to those exemplified for **18**. MS (ES^+): *m/z* 362.0 [M + 1].

4-(4-(2-Methyl-1H-imidazo[4,5-c]pyridin-1-yl)phenoxy)furo[3,2-c]pyridine (21). The title compound was prepared using methods closely related to those exemplified for **22** to afford **21** as a white solid in 90% yield. ^{1}H NMR (400 MHz, $CDCl_3$) δ 9.07 (s, 1H), 8.40 (d, *J* = 5.7 Hz,

1H), 8.07 (d, *J* = 5.9 Hz, 1H), 7.71 (d, *J* = 2.1 Hz, 1H), 7.52–7.47 (m, 2H), 7.45–7.40 (m, 2H), 7.30 (dd, *J* = 5.9, 0.8 Hz, 1H), 7.17 (dd, *J* = 5.6, 0.9 Hz, 1H), 6.98 (dd, *J* = 2.1, 0.8 Hz, 1H), 2.60 (s, 3H). ^{13}C NMR (126 MHz, $CDCl_3$) δ ppm 162.5, 157.1, 154.7, 153.6, 145.3, 142.7, 142.1, 141.8, 141.45, 140.0, 131.4, 128.2, 122.9, 113.6, 105.6, 104.8, 104.0, 14.7. MS (ES^+): *m/z* 343.1 [M + 1].

4-(3-Methyl-4-(2-methyl-1H-imidazo[4,5-c]pyridin-1-yl)phenoxy)furo[3,2-c]pyridine (22). A mixture of crude **16b** (from the preceding step, ≤14.7 mmol), **7** (2.37 g, 15.4 mmol) and cesium carbonate (99%, 19.3 g, 58.6 mmol) in DMSO (100 mL) was heated to 140 ºC for 16 h. After cooling to rt, the reaction mixture was diluted with EtOAc (400 mL) and filtered through a pad of Celite. The filtrate was washed with water, with a 1:1 mixture of water and saturated aq sodium chloride solution (4 x 100 mL), dried over sodium sulfate, filtered, and concd *in vacuo*. The residue was purified by silica gel chromatography (Gradient: 2% to 10% MeOH in EtOAc) to afford a yellow solid, which was dissolved in *tert*-butyl methyl ether (500 mL), treated with activated carbon (5 g), and heated to 40 ºC. The mixture was filtered to provide a colorless solution, which was concd at reflux until it became cloudy (~150 mL *tert*-butyl methyl ether remaining). Upon gradual cooling to rt, a precipitate formed. Filtration and washing with diethyl ether afforded **22** as a free-flowing white solid in 39% yield over 2 steps. ^{1}H NMR (500 MHz, $CDCl_3$) δ 9.08 (d, *J* = 1.0 Hz, 1H), 8.39 (d, *J* = 5.5 Hz, 1H), 8.08 (d, *J* = 5.9 Hz, 1H), 7.71 (d, *J* = 2.2 Hz, 1H), 7.36–7.34 (m, 1H), 7.30 (dd, *J* = 5.9, 1.0 Hz, 1H), 7.29–7.28 (m, 2H), 7.00 (dd, *J* = 5.5, 1.1 Hz, 1H), 6.97 (dd, *J* = 2.2, 1.0 Hz, 1H), 2.48 (s, 3H), 1.99 (br s, 3H). ^{13}C NMR (126 MHz, $CDCl_3$) δ ppm 162.4, 157.0, 155.1, 153.9, 145.3, 142.5, 142.0, 141.8, 141.2, 140.1, 137.9, 130.0, 129.4, 123.9, 120.3, 113.6, 105.6, 104.7, 103.9, 17.7, 14.3. MS (ES^+): 357.1 [M + 1].

4-(4-(6-Methoxyisoquinolin-5-yl)phenoxy)furo[3,2-c]pyridine (23). Compound **11a** (283 mg, 0.840 mmol), 5-bromo-6-methoxyisoquinoline (200 mg, 0.840 mmol), palladium acetate (9 mg,

0.084 mmol), triphenylphosphine (44 mg, 0.168 mmol), and potassium carbonate (232 mg, 1.68 mmol) were combined in a 2:1 mixture of dimethylformamide and water (1.5 mL) and heated at 80 ºC for 20 min. The reaction mixture was filtered through Celite; the filtrate was concd under reduced pressure, taken up in EtOAc, filtered through silica gel (1 g), and concd *in vacuo*. Purification via HPLC afforded **23** as a white solid in 9% yield. ^{1}H NMR (500 MHz, CD_3OD) δ 9.16 (s, 1H), 8.26 (d, *J* = 6.3 Hz, 1H), 8.21 (d, *J* = 9.0 Hz, 1H), 8.00 (d, *J* = 6.1 Hz, 1H), 7.90 (d, *J* = 2.2 Hz, 1H), 7.70 (d, *J* = 9.0 Hz, 1H), 7.52 (d, *J* = 6.3 Hz, 1H), 7.42–7.37 (m, 3H), 7.36–7.31 (m, 2H), 6.98–6.93 (m, 1H), 3.96 (s, 3H). MS (ES^+): *m/z* 369.0 [M + 1].

4-(4-(Imidazo[1,2-a]pyridin-5-yl)phenoxy)furo[3,2-c]pyridine (24). Compound **11a** (240 mg, 0.712 mmol), 5-bromoimidazo[1,2-*a*]pyridine (140 mg, 0.712 mmol), palladium acetate (16 mg, 0.071 mmol), triphenylphosphine (37 mg, 0.142 mmol), and potassium carbonate (197 mg, 1.42 mmol) were combined in a 3:1 mixture of DMF and water (4 mL) and heated at 70 ºC for 18 h. The reaction mixture was cooled to rt and poured into water (30 mL). The aq layer was extracted with EtOAc (3 x 50 mL). The combined organic layer was dried over sodium sulfate, filtered, and concd *in vacuo*; the residue was purified by silica gel chromatography (Eluent: EtOAc) to provide a light pink solid. The solid was loaded and eluted off of an ion exchange column to afford **24** as a white solid in 63% yield. ^{1}H NMR (400 MHz, $CDCl_3$) δ 8.07 (d, *J* = 5.8 Hz, 1H), 7.76–7.74 (m, 1H), 7.73–7.69 (m, 3H), 7.67–7.63 (m, 2H), 7.42 (br d, *J* = 8.6 Hz, 2H), 7.31–7.26 (m, 2H), 6.97 (dd, *J* = 2.2, 1.0 Hz, 1H), 6.79 (dd, *J* = 6.9, 1.1 Hz, 1H); MS (ES+): 328.0 [M + 1].

4-(4-(Imidazo[1,2-a]pyridin-5-yl)-3-methylphenoxy)furo[3,2-c]pyridine (25). Compound **11b** (50 mg, 0.140 mmol), 5-bromoimidazo[1,2-*a*]pyridine (33.5 mg, 0.170 mmol), [1,1′-bis(diphenylphosphino)ferrocene]dichloropalladium(II) (7 mg, 8 μmol), and potassium phosphate dihydrate (106 mg, 0.425 mmol) were combined in a 4:1 mixture of 2-methyltetrahydrofuran and water (1.25 mL) and heated at 75 ºC for 1 hour. After cooling to rt,

the reaction mixture was diluted with EtOAc (50 mL), dried over magnesium sulfate, filtered through Celite, and concd *in vacuo*. Purification via silica gel chromatography (Gradient: 0% to 100% EtOAc in heptane) afforded **25** as a solid in 62% yield. ^{1}H NMR (400 MHz, $CDCl_3$) δ 8.03 (d, *J* = 5.9 Hz, 1H), 7.65 (d, *J* = 2.3 Hz, 1H), 7.63 (br d, *J* = 9.2 Hz, 1H), 7.59 (d, *J* = 1.4 Hz, 1H), 7.35 (d, *J* = 8.2 Hz, 1H), 7.27–7.16 (m, 5H), 6.92 (dd, *J* = 2.1, 1.0 Hz, 1H), 6.70 (dd, *J* = 6.8, 1.0 Hz, 1H), 2.08 (s, 3H). MS (ES^+): 342.1 [M + 1].

4-(4-(6-Methylimidazo[1,2-a]pyridin-5-yl)phenoxy)furo[3,2-c]pyridine (26). A stirred mixture of 5-bromo-6-methylimidazo[1,2-*a*]pyridine[24b] (488 mg, 2.31 mmol), tetrakis(triphenylphosphine)palladium(0) (124 mg, 0.107 mmol), sodium carbonate (566 mg, 5.34 mmol), and **11a** (600 mg, 1.78 mmol) in a 1:3 mixture of EtOH and water (10 mL) was heated at 120 ºC in a microwave reactor for 30 min. The cooled reaction was diluted with EtOAc, filtered, and concd *in vacuo*. Purification via silica gel chromatography (mobile phase A: 100% DCM, mobile phase B: 20% MeOH in DCM; gradient: 0% to 40%) afforded **26** as a white solid in 63% yield. ^{1}H NMR (400 MHz, $CDCl_3$) δ 8.09 (d, *J* = 5.8 Hz, 1H), 7.70 (d, *J* = 2.2 Hz, 1H), 7.57 (br d, *J* = 9.2 Hz, 1H), 7.54 (d, *J* = 1.2 Hz, 1H), 7.49–7.43 (m, 4H), 7.29 (dd, *J* = 5.8, 1.0 Hz, 1H), 7.24–7.23 (m, 1H), 7.17 (d, *J* = 9.2 Hz, 1H), 6.96 (dd, *J* = 2.2, 1.0 Hz, 1H), 2.21 (s, 3H). ^{13}C NMR (126 MHz, DMSO-d_6) δ ppm 162.4, 157.3, 154.9, 147.2, 145.0, 142.4, 134.8, 133.7, 131.5, 129.8, 129.0, 122.9, 119.8, 116.6, 113.4, 111.8, 105.2, 104.3, 18.3. MS (ES^+): 342.1 [M + 1].

4-(3-Methyl-4-(6-methylimidazo[1,2-a]pyridin-5-yl)phenoxy)furo[3,2-c]pyridine (27). A stirred mixture of **11b** (75 mg, 0.210 mmol), 5-bromo-6-methylimidazo[1,2-*a*]pyridine[24b] (59 mg, 0.278 mmol), tetrakis(triphenylphosphine)palladium(0) (15 mg, 0.013 mmol), and sodium carbonate (113 mg, 1.07 mmol) in a 1:3 mixture of EtOH and water (4 mL) was heated at 120 ºC in a microwave reactor for 30 min. The cooled reaction was diluted with EtOAc, filtered through

Celite, and rinsed with EtOAc. The organic layer was washed with water and the resulting aq layer was extracted with EtOAc. The combined organic layer was dried, filtered, and concd *in vacuo*. Purification via silica gel chromatography (mobile phase A: 100% DCM, mobile phase B: 20% MeOH in DCM; gradient 0% to 40%) afforded **27** as a white solid in 79% yield. ^{1}H NMR (400 MHz, $CDCl_3$) δ 8.05 (d, J = 5.8 Hz, 1H), 7.65 (d, J = 2.3 Hz, 1H), 7.59–7.44 (m, 3H), 7.28–7.20 (m, 3H), 7.15 (d, J = 9.2 Hz, 1H), 7.00–6.95 (m, 1H), 6.90 (dd, J = 2.2, 1.0 Hz, 1H), 2.10 (s, 3H), 2.00 (s, 3H). MS (ES^+): 356.3 [M + 1].

4-(4-([1,2,4]Triazolo[1,5-a]pyrazin-5-yl)-3-methylphenoxy)furo[3,2-c]pyridine (28). A stirred mixture of **11b** (321 mg, 0.914 mmol), 5-bromo-[1,2,4]triazolo[1,5-*a*]pyrazine (140 mg, 0.703 mmol), tetrakis(triphenylphosphine)palladium(0) (83 mg, 0.070 mmol), and sodium carbonate (298 mg, 2.81 mmol) in a 1:2 mixture of water and dioxane (3 mL) was heated at 120 ºC in a microwave reactor for 1 h. The cooled reaction was diluted with EtOAc, filtered through Celite, and concd in vacuo. Purification via silica gel chromatography (Gradient: 0% to 100% EtOAc in heptanes) afforded **28** as a white solid in 68% yield. ^{1}H NMR (500 MHz, DMSO-d_6) δ 9.49 (s, 1H), 8.76 (s, 1H), 8.33 (s, 1H), 8.17 (d, J = 2.2 Hz, 1H), 8.03 (d, J = 5.9 Hz, 1H), 7.58 (d, J = 8.3 Hz, 1H), 7.51 (dd, J = 5.9, 1.0 Hz, 1H), 7.32 (d, J = 2.2 Hz, 1H), 7.24 (dd, J = 8.5, 2.4 Hz, 1H), 7.15 (dd, J = 2.2, 1.0 Hz, 1H), 2.12 (s, 3H). MS (ES^+): 357.0 [M + 1].

4-(3-Methyl-4-(6-methylimidazo[1,2-a]pyrazin-5-yl)phenoxy)furo[3,2-c]pyridine (29). A stirred mixture of **11b** (100 mg, 0.285 mmol), 5-bromo-6-methylimidazo[1,2-*a*]pyrazine[24b] (70 mg, 0.330 mmol), tetrakis(triphenylphosphine)palladium(0) (157 mg, 0.015 mmol), and sodium carbonate (80 mg, 0.750 mmol) in a 1:3 mixture of EtOH and water (2.7 mL) was heated at 120 ºC in a microwave reactor for 1.5 hours. The cooled reaction was filtered through Celite and concd *in vacuo* to a dark oil. Purification via silica gel chromatography (Gradient: 0% to 5% MeOH in EtOAc) afforded **29** as an off-white solid in 46% yield. ^{1}H NMR (500 MHz, $CDCl_3$) δ

9.15 (s, 1H), 8.09 (d, *J* = 5.9 Hz, 1H), 7.76 (d, *J* = 1.2 Hz, 1H), 7.70 (d, *J* = 2.2 Hz, 1H), 7.36–7.26 (m, 4H), 7.19 (s, 1H), 6.96 (dd, *J* = 2.2, 1.0 Hz, 1H), 2.40 (s, 3H), 2.07 (s, 3H). ^{13}C NMR (101 MHz, $CDCl_3$) δ 162.2, 157.0, 155.3, 144.9, 141.7, 141.7, 140.2, 139.2, 136.2, 135.5, 130.9, 127.1, 127.0, 132.2, 119.6, 113.5, 112.3, 104.4, 103.8, 20.1, 19.0. MS (ES^+): 357.0 [M + 1]. mp = 165.6 °C.

(-)-4-(3-methyl-4-(6-methylimidazo[1,2-a]pyrazin-5-yl)phenoxy)furo[3,2-c]pyridine (30) and (+)-4-(3-Methyl-4-(6-methylimidazo[1,2-a]pyrazin-5-yl)phenoxy)furo[3,2-c]pyridine (31). Racemic **29** was separated into its atropo-enantiomers using supercritical fluid chromatography[30] (Column: Chiralpak AD-H, 5 μm; Eluent: 3:1 carbon dioxide / MeOH). (+)-Enantiomer **31** was the first-eluting isomer, followed by (−)-enantiomer **30**. Compound 30:$[\alpha]^{20}_D$ -30.9 (*c* 0.35, CH_2Cl_2), >98% *ee*. Compound 31:$[\alpha]^{20}_D$ +35.2 (*c* 0.32, CH_2Cl_2), >98% *ee*. For data supporting the absolute stereochemistry of both enantiomers including VCD and small molecule X-ray crystal structure please see the supporting information.

Acknowledgements:

We would like to acknowledge Scot Mente and Elizabeth Collantes for computational modelling support and helpful discussions, Lois Chenard and our Wuxi team for technical assistance in running libraries, Tony Yan and Laurence Phillip for analytical support, Mark Bundesmann for experimental assistance characterizing atropisomer racemization kinetics, Andrew Flick, Bruce Rogers, Patrick Verhoest, Anabella Villalobos and Donn Wishka for helpful discussions, and Katherine Brighty and Katherine Lee for assistance in manuscript preparation.

AUTHOR INFORMATION

Corresponding Author

* E-mail jennifer.e.davoren@pfizer.com

The authors declare no competing financial interest.

Abbreviations

Dopamine (DA), central nervous system (CNS), Parkinson's disease (PD), intravenously (IV), positive allosteric modulators (PAMs), high-throughput screen (HTS), homogenous time-resolved fluorescence (HTRF), human embryonic kidney (HEK), human D1 (hD1), human D1 receptor (hD1r), structure-activity relationship (SAR), matched molecular pair (MMP), multi-parameter optimization (MPO), multidrug resistance protein (MDR), breast cancer resistance protein (BCRP), polar surface area (PSA), hydrogen bond donor (HBD), area under the curve (AUC), human liver microsome (HLM), human hepatocyte (hHep), lipophilic efficiency (LipE), pharmacokinetics (PK), locomotor activity (LMA), brain/plasma (B/P), fraction unbound in brain ($F_{b,u}$), fraction unbound in plasma ($F_{p,u}$), concentration unbound in brain ($C_{b,u}$), and concentration unbound in plasma ($C_{p,u}$).

Associated Content

Supporting Information: The supporting information is available free of charge on the ACS publications website. Included are purity report of compound **29**; PXRD, purity report, X-ray structure data for compound **31**; VCD, raw data, calculation, and analysis of compound **30** racemization kinetics; biological methods for locomotor and desensitization assays; methods for the D1 radioligand binding and cAMP functional assays; molecular smiles strings for all final compounds.

References

1. (a) Schulz, D. W.; Stanford, E. J.; Wyrick, S. W.; Mailman, R. B. Binding of [3H]SCH23390 in rat brain: regional distribution and effects of assay conditions and GTP suggest interactions at

a D1-like dopamine receptor. *J. Neurochem.* **1985,** *45,* 1601-1611; (b) Beaulieu, J. M.; Gainetdinov, R. R. The physiology, signaling, and pharmacology of dopamine receptors. *Pharmacol. Rev.* **2011,** *63,* 182-217.

2. Missale, C.; Nash, S. R.; Robinson, S. W.; Jaber, M.; Caron, M. G. Dopamine receptors: from structure to function. *Physiol. Rev.* **1998,** *78,* 189-225.

3. Kebabian, J. W.; Petzold, G. L.; Greengard, P. Dopamine-sensitive adenylate cyclase in caudate nucleus of rat brain, and its similarity to the "dopamine receptor". *Proc. Natl. Acad. Sci. U.S.A.* **1972,** *69,* 2145-2149.

4. (a) Abi-Dargham, A.; Moore, H. Prefrontal DA transmission at D1 receptors and the pathology of schizophrenia. *Neuroscientist* **2003,** *9,* 404-416; (b) Goldman-Rakic, P. S.; Castner, S. A.; Svensson, T. H.; Siever, L. J.; Williams, G. V. Targeting the dopamine D1 receptor in schizophrenia: insights for cognitive dysfunction. *Psychopharmacology (Berl)* **2004,** *174,* 3-16; (c) Huang, Y. Y.; Kandel, E. R. D1/D5 receptor agonists induce a protein synthesis-dependent late potentiation in the CA1 region of the hippocampus. *Proc. Natl. Acad. Sci. U.S.A.* **1995,** *92,* 2446-2450; (d) Huang, Y. Y.; Simpson, E.; Kellendonk, C.; Kandel, E. R. Genetic evidence for the bidirectional modulation of synaptic plasticity in the prefrontal cortex by D1 receptors. *Proc. Natl. Acad. Sci. U.S.A.* **2004,** *101,* 3236-3241; (e) Williams, G. V.; Castner, S. A. Under the curve: critical issues for elucidating D1 receptor function in working memory. *Neuroscience* **2006,** *139,* 263-276.

5. Gerfen, C. R.; Engber, T. M. Molecular neuroanatomic mechanisms of Parkinson's disease: a proposed therapeutic approach. *Neurologic clinics* **1992,** *10,* 435-449.

6. (a) Abi-Dargham, A.; Mawlawi, O.; Lombardo, I.; Gil, R.; Martinez, D.; Huang, Y.; Hwang, D. R.; Keilp, J.; Kochan, L.; Van Heertum, R.; Gorman, J. M.; Laruelle, M. Prefrontal dopamine D1 receptors and working memory in schizophrenia. *J. Neurosci.* **2002,** *22,* 3708-3719; (b)

Davis, K. L.; Kahn, R. S.; Ko, G.; Davidson, M. Dopamine in schizophrenia: a review and reconceptualization. *Am. J. Psychiatry* **1991,** *148,* 1474-1486; (c) Gao, W. J.; Wang, Y.; Goldman-Rakic, P. S. Dopamine modulation of perisomatic and peridendritic inhibition in prefrontal cortex. *J. Neurosci.* **2003,** *23,* 1622-1630; (d) Goldman-Rakic, P. S.; Muly, E. C., 3rd; Williams, G. V. D(1) receptors in prefrontal cells and circuits. *Brain Res. Rev.* **2000,** *31,* 295-301; (e) Gonzalez-Islas, C.; Hablitz, J. J. Dopamine enhances EPSCs in layer II-III pyramidal neurons in rat prefrontal cortex. *J. Neurosci.* **2003,** *23,* 867-875; (f) Goulet, M.; Madras, B. K. D(1) dopamine receptor agonists are more effective in alleviating advanced than mild parkinsonism in 1-methyl-4-phenyl-1,2,3, 6-tetrahydropyridine-treated monkeys. *J. Pharmacol. Exp. Ther.* **2000,** *292,* 714-724; (g) Seamans, J. K.; Gorelova, N.; Durstewitz, D.; Yang, C. R. Bidirectional dopamine modulation of GABAergic inhibition in prefrontal cortical pyramidal neurons. *J. Neurosci.* **2001,** *21,* 3628-3638; (h) Weinberger, D. R. Implications of normal brain development for the pathogenesis of schizophrenia. *Arch. Gen. Psychiatry* **1987,** *44,* 660-669; (i) Goto, Y.; O'Donnell, P. Synchronous activity in the hippocampus and nucleus accumbens in vivo. *J. Neurosci.* **2001,** *21,* RC131; (j) Goto, Y.; O'Donnell, P. Network synchrony in the nucleus accumbens in vivo. *J. Neurosci.* **2001,** *21,* 4498-4504; (k) Goto, Y.; O'Donnell, P. Delayed mesolimbic system alteration in a developmental animal model of schizophrenia. *J. Neurosci.* **2002,** *22,* 9070-9077; (l) Taylor, J. R.; Lawrence, M. S.; Redmond, D. E., Jr.; Elsworth, J. D.; Roth, R. H.; Nichols, D. E.; Mailman, R. B. Dihydrexidine, a full dopamine D1 agonist, reduces MPTP-induced parkinsonism in monkeys. *Eur. J. Pharmacol.* **1991,** *199,* 389-391; (m) Lewis, M. M.; Huang, X.; Nichols, D. E.; Mailman, R. B. D1 and functionally selective dopamine agonists as neuroprotective agents in Parkinson's disease. *CNS & neurological disorders drug targets* **2006,** *5,* 345-353; (n) Mailman, R.; Huang, X.; Nichols, D. E. Parkinson's

disease and D1 dopamine receptors. *Current opinion in investigational drugs* **2001,** *2,* 1582-1591.

7. (a) Ye, N.; Neumeyer, J. L.; Baldessarini, R. J.; Zhen, X.; Zhang, A. Update 1 of: Recent progress in development of dopamine receptor subtype-selective agents: potential therapeutics for neurological and psychiatric disorders. *Chem. Rev.* **2013,** *113,* PR123-178; (b) Zhang, J.; Xiong, B.; Zhen, X.; Zhang, A. Dopamine D1 receptor ligands: where are we now and where are we going. *Medicinal research reviews* **2009,** *29,* 272-294.

8. (a) Pendleton, R. G.; Samler, L.; Kaiser, C.; Ridley, P. T. Studies on renal dopamine receptors with a new agonist. *Eur. J. Pharmacol.* **1978,** *51,* 19-28; (b) Setler, P. E.; Sarau, H. M.; Zirkle, C. L.; Saunders, H. L. The central effects of a novel dopamine agonist. *Eur. J. Pharmacol.* **1978,** *50,* 419-430; (c) Mottola, D. M.; Brewster, W. K.; Cook, L. L.; Nichols, D. E.; Mailman, R. B. Dihydrexidine, a novel full efficacy D1 dopamine receptor agonist. *J. Pharmacol. Exp. Ther.* **1992,** *262,* 383-393; (d) Ghosh, D.; Snyder, S. E.; Watts, V. J.; Mailman, R. B.; Nichols, D. E. 9-Dihydroxy-2,3,7,11b-tetrahydro-1H-naph[1,2,3-de]isoquinoline: a potent full dopamine D1 agonist containing a rigid-beta-phenyldopamine pharmacophore. *J. Med. Chem.* **1996,** *39,* 549-555.

9. (a) Kebabian, J. W.; Britton, D. R.; DeNinno, M. P.; Perner, R.; Smith, L.; Jenner, P.; Schoenleber, R.; Williams, M. A-77636: a potent and selective dopamine D1 receptor agonist with antiparkinsonian activity in marmosets. *Eur. J. Pharmacol.* **1992,** *229,* 203-209; (b) Kebabian, J. W.; DeNinno, M. P.; Schoenleber, R.; MacKenzie, R.; Britton, D. R.; Asin, K. E. A68930: a potent agonist specific for the dopamine D1 receptor. *Neurochem. Int.* **1992,** *20 Suppl,* 157S-160S; (c) DeNinno, M. P.; Schoenleber, R.; MacKenzie, R.; Britton, D. R.; Asin, K. E.; Briggs, C.; Trugman, J. M.; Ackerman, M.; Artman, L.; Bednarz, L.; et al. A68930: a potent agonist selective for the dopamine D1 receptor. *Eur. J. Pharmacol.* **1991,** *199,* 209-219; (d)

Snyder, S. E.; Aviles-Garay, F. A.; Chakraborti, R.; Nichols, D. E.; Watts, V. J.; Mailman, R. B. Synthesis and evaluation of 6,7-dihydroxy-2,3,4,8,9,13b-hexahydro-1H-benzo[6,7]cyclohepta[1,2,3-ef][3]benzazepine, 6,7-dihydroxy- 1,2,3,4,8,12b-hexahydroanthr[10,4a,4-cd]azepine, and 10-(aminomethyl)-9,10- dihydro-1,2-dihydroxyanthracene as conformationally restricted analogs of beta-phenyldopamine. *J. Med. Chem.* **1995,** *38,* 2395-2409; (e) Andersen, P. H.; Jansen, J. A. Dopamine receptor agonists: selectivity and dopamine D1 receptor efficacy. *Eur. J. Pharmacol.* **1990,** *188,* 335-347.

10. (a) Dubois, A.; Savasta, M.; Curet, O.; Scatton, B. Autoradiographic distribution of the D1 agonist [3H]SKF 38393, in the rat brain and spinal cord. Comparison with the distribution of D2 dopamine receptors. *Neuroscience* **1986,** *19,* 125-137; (b) Weed, M. R.; Vanover, K. E.; Woolverton, W. L. Reinforcing effect of the D1 dopamine agonist SKF 81297 in rhesus monkeys. *Psychopharmacology (Berl)* **1993,** *113,* 51-52.

11. Arnsten, A. F.; Girgis, R. R.; Gray, D. L.; Mailman, R. B. Novel dopamine therapeutics for cognitive deficits in Schizophrenia. *Biological psychiatry* **2017,** *81,* 67-77.

12. Grenader, A.; Healy, D. P. Fenoldopam is a partial agonist at dopamine-1 (DA1) receptors in LLC-PK1 cells. *J. Pharmacol. Exp. Ther.* **1991,** *258,* 193-198.

13. Andersen, P. H.; Nielsen, E. B.; Scheel-Kruger, J.; Jansen, J. A.; Hohlweg, R. Thienopyridine derivatives identified as the first selective, full efficacy, dopamine D1 receptor agonists. *Eur. J. Pharmacol.* **1987,** *137,* 291-292.

14. Brogden, R. N.; Markham, A. Fenoldopam: a review of its pharmacodynamic and pharmacokinetic properties and intravenous clinical potential in the management of hypertensive urgencies and emergencies. *Drugs* **1997,** *54,* 634-650.

15. Gray, D. L.; Allen, J. A.; Mente, S.; O'Connor, R. E.; DeMarco, G. J.; Efremov, I.; Tierney, P.; Volfson, D.; Davoren, J.; Guilmette, E.; Salafia, M.; Kozak, R.; Ehlers, M. D. Impaired beta-

arrestin recruitment and reduced desensitization by non-catechol agonists of the D1 dopamine receptor. *Nat. Commun.* **2018,** *9,* 674.

16. (a) Lewis, M. A.; Hunihan, L.; Watson, J.; Gentles, R. G.; Hu, S.; Huang, Y.; Bronson, J.; Macor, J. E.; Beno, B. R.; Ferrante, M.; Hendricson, A.; Knox, R. J.; Molski, T. F.; Kong, Y.; Cvijic, M. E.; Rockwell, K. L.; Weed, M. R.; Cacace, A. M.; Westphal, R. S.; Alt, A.; Brown, J. M. Discovery of D1 dopamine receptor positive allosteric modulators: characterization of pharmacology and identification of residues that regulate species selectivity. *J. Pharmacol. Exp. Ther.* **2015,** *354,* 340-349; (b) Wang, X.; Heinz, B. A.; Qian, Y. W.; Carter, J. H.; Gadski, R. A.; Beavers, L. S.; Little, S. P.; Yang, C. R.; Beck, J. P.; Hao, J.; Schaus, J. M.; Svensson, K. A.; Bruns, R. F. Intracellular binding site for a positive allosteric modulator of the dopamine D1 receptor. *Mol. Pharmacol.* **2018,** *94,* 1232-1245.

17. Kawakami, S.; Imaizumi, T.; Masuda, N.; Kunikawa, S.; Morita, M.; Yarimizu, J. Preparation of Imidazodiazepine Compounds as Dopamine D1 Receptor Positive Allosteric Modulators (D1 PAM). WO 2016204268, 2016.

18. Eglen, R. M. An overview of high throughput screening at G protein coupled receptors. *Frontiers in Drug Design & Discovery* **2005,** *1,* 97-111.

19. Sibley, D. R.; Leff, S. E.; Creese, I. Interactions of novel dopaminergic ligands with D-1 and D-2 dopamine receptors. *Life Sci.* **1982,** *31,* 637-645.

20. Schiff, P. L. Ergot and its alkaloids. *American journal of pharmaceutical education* **2006,** *70,* 98.

21. Billard, W.; Ruperto, V.; Crosby, G.; Iorio, L. C.; Barnett, A. Characterization of the binding of 3H-SCH 23390, a selective D-1 receptor antagonist ligand, in rat striatum. *Life Sci.* **1984,** *35,* 1885-1893.

22. (a) Baell, J.; Walters, M. A. Chemistry: Chemical con artists foil drug discovery. *Nature* **2014,** *513,* 481-483; (b) Baell, J. B.; Holloway, G. A. New substructure filters for removal of pan assay interference compounds (PAINS) from screening libraries and for their exclusion in bioassays. *J. Med. Chem.* **2010,** *53,* 2719-2740.

23. Chein, R. J.; Corey, E. J. Strong conformational preferences of heteroaromatic ethers and electron pair repulsion. *Org. Lett.* **2010,** *12,* 132-135.

24. (a) Wang, Z.; Chi, Y.; Harris, A. R.; Gray, D.; Davoren, J. E. Scalable synthesis of 4-substituted 5-bromo-6-methylpyrimidines. *Synthesis* **2011,** 1529-1531; (b) Harris, A. R.; Nason, D. M.; Collantes, E. M.; Xu, W.; Chi, Y.; Wang, Z.; Zhang, B.; Zhang, Q.; Gray, D. L.; Davoren, J. E. Synthesis of 5-bromo-6-methyl imidazopyrazine, 5-bromo and 5-chloro-6-methyl imidazopyridine using electron density surface maps to guide synthetic strategy. *Tetrahedron* **2011,** *67,* 9063-9066.

25. Coe, J. W.; Allen, J. A.; Davoren, J. E.; Dounay, A. B.; Efremov, I. V.; Gray, D. L. F.; Guilmette, E. R.; Harris, A. R.; Helal, C. J.; Henderson, J. L.; Mente, S. R.; Nason, D. M., II; O'Neil, S. V.; Subramanyam, C.; Xu, W. Preparation of Heteroaromatic Compounds and their use as Dopamine D1 Ligands for Therapy. WO 2014072881 2013.

26. Griffen, E.; Leach, A. G.; Robb, G. R.; Warner, D. J. Matched molecular pairs as a medicinal chemistry tool. *J. Med. Chem.* **2011,** *54,* 7739-7750.

27. (a) Ryckmans, T.; Edwards, M. P.; Horne, V. A.; Correia, A. M.; Owen, D. R.; Thompson, L. R.; Tran, I.; Tutt, M. F.; Young, T. Rapid assessment of a novel series of selective CB(2) agonists using parallel synthesis protocols: A Lipophilic Efficiency (LipE) analysis. *Bioorg. Med. Chem. Lett.* **2009,** *19,* 4406-4409; (b) Johnson, T. W.; Gallego, R. A.; Edwards, M. P. Lipophilic efficiency as an important metric in drug design. *J. Med. Chem.* **2018,** *61,* 6401-6420.

28. (a) Laplante, S. R.; L, D. F.; Fandrick, K. R.; Fandrick, D. R.; Hucke, O.; Kemper, R.; Miller, S. P.; Edwards, P. J. Assessing atropisomer axial chirality in drug discovery and development. *J. Med. Chem.* **2011,** *54,* 7005-7022; (b) Clayden, J.; Moran, W. J.; Edwards, P. J.; LaPlante, S. R. The challenge of atropisomerism in drug discovery. *Angew. Chem. Int. Ed. Engl.* **2009,** *48,* 6398-6401.

29. Compound 22 is a confirmed racemic mixture of two stable atropisomers.

30. Yan, T. Q.; Riley, F.; Philippe, L.; Davoren, J.; Cox, L.; Orozco, C.; Rai, B.; Hardink, M. Chromatographic resolution of atropisomers for toxicity and biotransformation studies in pharmaceutical research. *J. Chromatogr. A* **2015,** *1398,* 108-120.

31. For an explanation on nomenclature see: 1. Bringmann, G.; Price Mortimer, A. J.; Keller, P. A.; Gresser, M. J.; Garner, J.; Breuning, M. Atroposelective synthesis of axially chiral biaryl compounds. Angew. Chem. Int. Ed. Engl. 2005, 44, 5384-5427.

32. Hooft, R. W.; Straver, L. H.; Spek, A. L. Determination of absolute structure using Bayesian statistics on Bijvoet differences. *J. Appl. Crystallogr.* **2008,** *41,* 96-103.

33. Freedman, T. B.; Cao, X.; Dukor, R. K.; Nafie, L. A. Absolute configuration determination of chiral molecules in the solution state using vibrational circular dichroism. *Chirality* **2003,** *15,* 743-758.

34. Davoren, J. E.; Bundesmann, M. W.; Yan, Q. T.; Collantes, E. M.; Mente, S.; Nason, D. M.; Gray, D. L. Measurement of atropisomer racemization kinetics using segmented flow technology. *ACS Med. Chem. Lett.* **2012,** *3,* 433-435.

35. Shi, Y.; Huang, M. H.; Macor, J. E.; Hughes, D. E. Characterization of the in vitro atropisomeric interconversion rates of an endothelin A antagonist by enantioselective liquid chromatography. *J. Chromatogr. A* **2005,** *1078,* 67-73.

36. Lombardo, F.; Shalaeva, M. Y.; Tupper, K. A.; Gao, F. ElogD(oct): a tool for lipophilicity determination in drug discovery. 2. Basic and neutral compounds. *J. Med. Chem.* **2001,** *44,* 2490-2497.

37. Goetz, G. H.; Philippe, L.; Shapiro, M. J. EPSA: A novel supercritical fluid chromatography technique enabling the design of permeable cyclic peptides. *ACS Med. Chem. Lett.* **2014,** *5,* 1167-1172.

38. Wager, T. T.; Hou, X.; Verhoest, P. R.; Villalobos, A. Moving beyond rules: the development of a central nervous system multiparameter optimization (CNS MPO) approach to enable alignment of druglike properties. *ACS Chem. Neurosci.* **2010,** *1,* 435-449.

39. Zhou, L.; Schmidt, K.; Nelson, F. R.; Zelesky, V.; Troutman, M. D.; Feng, B. The effect of breast cancer resistance protein and P-glycoprotein on the brain penetration of flavopiridol, imatinib mesylate (Gleevec), prazosin, and 2-methoxy-3-(4-(2-(5-methyl-2-phenyloxazol-4-yl)ethoxy)phenyl)propanoic acid (PF-407288) in mice. *Drug. Metab. Dispos.* **2009,** *37,* 946-955.

40. Di, L.; Whitney-Pickett, C.; Umland, J. P.; Zhang, H.; Zhang, X.; Gebhard, D. F.; Lai, Y.; Federico, J. J., 3rd; Davidson, R. E.; Smith, R.; Reyner, E. L.; Lee, C.; Feng, B.; Rotter, C.; Varma, M. V.; Kempshall, S.; Fenner, K.; El-Kattan, A. F.; Liston, T. E.; Troutman, M. D. Development of a new permeability assay using low-efflux MDCKII cells. *J. Pharm. Sci.* **2011,** *100,* 4974-4985.

41. Riccardi, K.; Cawley, S.; Yates, P. D.; Chang, C.; Funk, C.; Niosi, M.; Lin, J.; Di, L. Plasma protein binding of challenging compounds. *J. Pharm. Sci.* **2015,** *104,* 2627-2636.

42. (a) Thomsen, M.; Ralph, R. J.; Caine, S. B. Psychomotor stimulation by dopamine D(1)-like but not D(2)-like agonists in most mouse strains. *Experimental and clinical psychopharmacology* **2011,** *19,* 342-360; (b) Desai, R. I.; Terry, P.; Katz, J. L. A comparison of the locomotor

stimulant effects of D1-like receptor agonists in mice. *Pharmacol. Biochem. Behav.* **2005,** *81,* 843-848.

43. 7-chloro-3-methyl-1-phenyl-1,2,4,5-tetrahydro-3-benzazepin-8-ol

44. Rivera, A.; Alberti, I.; Martin, A. B.; Narvaez, J. A.; de la Calle, A.; Moratalla, R. Molecular phenotype of rat striatal neurons expressing the dopamine D5 receptor subtype. *Eur. J. Neurosci.* **2002,** *16,* 2049-2058.

45. (1R,3S)-3-(1-Adamantyl)-1-(aminomethyl)-3,4-dihydro-1H-isochromene-5,6-diol (A77636)

46. 6-Chloro-3-methyl-1-(3-methylphenyl)-2,3,4,5-tetrahydro-1H-3-benzazepine-7,8-diol (SKF-83959)

Table of Contents Graphic

HTS Hit

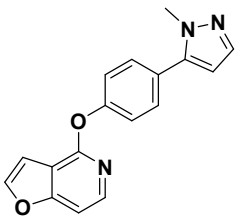

PF-4211 (6)
D1 EC_{50} (cAMP): 2.3 μM, 37% emax
D1 Binding K_i: 2.2 μM

Atropisomer Lead

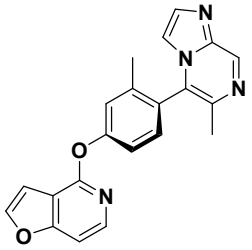

PF-06256142 (31)
D1 EC_{50} (cAMP): 33 nM, 91% emax
D1 Binding K_i: 12 nM